NASA Technical Paper 1455

The Use of Computer-Generated Color Graphic Images for Transient Thermal Analysis

C. L. W. Edwards, Frances T. Meissner,
and James B. Hall

JULY 1979

NASA

NASA Technical Paper 1455

The Use of Computer-Generated Color Graphic Images for Transient Thermal Analysis

C. L. W. Edwards, Frances T. Meissner,
and James B. Hall
Langley Research Center
Hampton, Virginia

National Aeronautics
and Space Administration

**Scientific and Technical
Information Branch**

1979

SUMMARY

Color computer graphics techniques were investigated as a means of rapidly scanning and interpreting large sets of transient heating data. The data presented in this paper were generated to support the conceptual design of a heat-sink thermal protection system (TPS) for a hypersonic research airplane. Color-coded vector and raster displays of the numerical geometry used in the heating calculations were employed to analyze skin thicknesses and surface temperatures of the heat-sink TPS under a variety of trajectory flight profiles. Both vector and raster displays proved to be effective means for rapidly identifying heat-sink mass concentrations, regions of high heating, and potentially adverse thermal gradients. The color-coded (raster) surface displays are a very efficient means for displaying surface-temperature and heating histories, and thereby the more stringent design requirements can quickly be identified. The related hardware and software developments required to implement both the vector and the raster displays for this application are also discussed.

INTRODUCTION

Thermal protection systems (TPS), which are essential to the ultimate flight safety of high-speed aircraft, can comprise a large percentage of the vehicle dry weight. The actual percentage depends on the vehicle mission requirements and type of TPS employed; however, the TPS weight can easily be equal to or greater than the payload weight for flight Mach numbers greater than 5. Therefore, the vehicle TPS must be considered throughout the configuration design if vehicle performance is to be maximized to any real degree for high Mach number missions. If such a design approach is adopted, then the level of effort devoted to thermal analysis can be comparable with the level of effort devoted to other major design disciplines (e.g., aerodynamics, propulsion, and primary structure), since effective trade-offs generally require consistency in accuracy.

The application of extended thermal analysis during conceptual design is well illustrated by recent studies to define a hypersonic research airplane (refs. 1, 2, 3, and 4). Investigations into the feasibility of using a heat-sink TPS over a broad high-speed flight envelope were an integral part of these studies. Transient heating analyses over the vehicle surface for several skin materials (refs. 2 and 4), vehicle configurations (refs. 1, 2, 3, and 4), and flight profiles (refs. 2, 3, and 4) were conducted and led to the development of rapid means for (1) making the transient heating calculations and (2) scanning and interpreting the large volume of data generated so that the heating calculations would effectively impact the design. Summary results of the method used for rapid transient heating calculations over the complete vehicle were presented in reference 4. The approach to the problem of rapid interpretation of the transient heating data is the primary subject of this paper.

Use of trade names or names of manufacturers in this paper does not constitute an endorsement of such products or manufacturers, either expressed or implied, by the National Aeronautics and Space Administration.

SYMBOLS

A	area of surface panel of interest
B_1, B_2, B_3, B_4, B_5	coefficients to represent specific heat of skin material as a function of surface temperature
C_p	heat capacity of heat-sink skin material
h	heat transfer coefficient
k	coefficient of thermal conductivity
M_{max}	Mach number of maximum dash capability of vehicle
M_∞	free-stream Mach number
Q_{acc}	running sum of vehicle heat load per trajectory
q_∞	free-stream dynamic pressure
T_{avg}	area-weighted average vehicle surface temperature
T_i	assumed initial vehicle surface temperature
T_{limit}	maximum allowable working temperature of material used for heat-sink skin
T_{loc}	local surface temperature at any given trajectory flight condition
T_{max}	maximum vehicle surface temperature at any given trajectory flight condition
T_{min}	minimum vehicle surface temperature at any given trajectory flight condition
T_R	recovery temperature
T_s	panel surface temperature at any given trajectory flight condition
$T_{s,t-\Delta t}$	panel surface temperature at previous trajectory flight condition
t	trajectory flight time
t_i	trajectory flight time when $M_\infty = 2$, where transient heating calculations were initiated

α vehicle angle of attack

Δt elapsed time between current and previous trajectory heat calculation points

$\varepsilon_1, \varepsilon_2$ outer and inner panel surface emissivity, respectively

ρ density of heat-sink skin material

σ Stefan-Boltzman constant for radiation heating

τ panel thickness

Abbreviations:

CPU central processor unit

CRT cathode ray tube

RDU raster display unit

RGB red-green-blue

TPS thermal protection system

TPS CONCEPTUAL DESIGN METHOD

Because TPS weight greatly affects performance in a heat-sink concept, the basic design objective was to minimize this weight (or maximize performance) over the widest possible flight envelope without compromising structural integrity. The primary TPS design variables are associated with the structural concept, the heat-sink material physical properties, and the mission profile. Finite-element analysis of a structure with a heat-sink TPS would indicate possible regions where thermal stresses exceed the effects due to pressure loads (ref. 3). However, extensive application of large finite-element models to a wide variety of flight conditions and material and geometric configurations is not consistent with the conceptual design process. Such calculations are usually relied on to evaluate and refine a given configuration. Therefore, a new approach was sought to rapidly estimate the heat-sink mass distribution and transient heating over the entire vehicle surface. This information could then be used effectively to improve early performance estimates and to identify potential areas of significant thermal stress requiring more comprehensive analysis to complete the design.

The approach employed in this TPS conceptual design study was to estimate the vehicle thermal response by calculating the transient heating to a number of panels distributed over the vehicle surface as shown in figure 1. This distribution of the surface panels represents a nearly minimum set required to retain accuracy in both surface gradients and integrated heating values. The type of heating calculations performed on individual panels is illustrated in figure 2. Convective heating to the exterior surface was approximated through

Spalding-Chi estimates of local skin friction. Heat was allowed to radiate away from the panel, but not to the internal structure. Likewise, conduction out of the plate edges or through structural members was assumed to be zero to insure a conservative estimate of heating. Thus, the heat-balance equation is

$$\rho C_p \tau A\left(\frac{T_s - T_{s,t-\Delta t}}{\Delta t}\right) = h(T_R - T_s)A - \sigma\varepsilon_1 T_s^4 A$$

where

$$C_p = B_1 + B_2 T_s + B_3 T_s^2 + B_4 T_s^3 + B_5 T_s^4$$

Throughout the study, all convective heating rates were increased by 25 percent as a design safety factor. The panel thickness was used to control the maximum temperature over any given trajectory. Vehicle performance was iteratively optimized by considering the influence of changes in trajectory and vehicle weight due to panel thickness while allowing each panel to reach but not exceed a specified maximum material temperature. Approximately 50 000 panel calculations were required to optimize the performance of the vehicle and its TPS over a given trajectory (i.e., 200 panels for approximately 8 combinations of thickness and local surface temperatures at about 30 flight conditions). These calculations were very rapid, requiring less than 100 sec of CPU time per mission on a CDC 6600 computer, and effects on performance could easily be evaluated.

Typical trajectory profiles for the two limiting missions for TPS design are illustrated in figure 3. Figure 3(a) presents histories of the free-stream Mach number, vehicle angle of attack, and free-stream dynamic pressure for the maximum Mach number dash mission. Flight speeds in excess of Mach 2 were considered necessary to significantly alter the heat load to the vehicle, so that heating calculations were begun at $M_\infty = 2$. The circular symbols indicate data points used to establish the transient heat history. The equivalent trajectory profiles for 120 sec of cruise at Mach 6 mission are presented in figure 3(b). These two flight trajectories are realistic for the configuration shown in figure 1 when Lockalloy (a 62-percent-beryllium and 38-percent-aluminum alloy) is used for the vehicle skin. The histories of vehicle integrated heat loads for these two trajectories are presented in figure 4. The total heat absorbed for the dash mission is almost identical to that for the 120 sec of cruise mission, so that these two trajectories represent good design evaluation criteria from the standpoint of maximum vehicle performance. A history of 60 sec of cruise at Mach 6 mission is also presented as a representative minimum vehicle performance constraint. A more comprehensive summary of performance for four different materials (beryllium, titanium, Lockalloy, and aluminum) and combinations thereof during a variety of anticipated research airplane missions is presented in reference 4.

The identification of potential thermal stress problems which can occur anytime throughout the mission requires at least a cursory knowledge of the

heating and the temperature gradients over the surface. This type of information is available through the panel transient heating calculations; however, interpreting the tremendous volume of data associated with vehicle, material, and mission parameters is no small task. Therefore, during the TPS design study, a means of rapid interpretation of thermal data also became an analytical goal. The use of color graphics on the vehicle geometry to represent the data available from the heating calculations proved to be very effective. The remainder of this paper primarily illustrates the effectiveness of this technique and describes the associated research required for its implementation. In the next section the development of color graphics software and hardware in support of the TPS design study is summarized.

COLOR GRAPHICS APPROACHES

There are several black and white, intensity (or contrast) oriented computer graphic techniques which can represent the variation of a scalar parameter (e.g., skin thickness or surface temperature) on the surface of a three-dimensional object (e.g., a research aircraft). It was decided early in the TPS design study that none of these techniques could truly produce the desired result unless color was used to code the data, that is, unless a set of distinguishable colors were associated with the discrete values assumed by the scalar parameter as it varies on the surface. The decision to use color severely limited the types of display devices available.

Since the analysis programs used to produce the TPS data for graphic display were already organized to produce vector graphic (i.e., wire frame) output and since an Adage vector graphics terminal with limited color capability was available, it was decided to evaluate the use of this system to support the TPS design study.

Color Vector Graphics

The Adage system has a main scope with three auxiliary scopes, each capable of generating an independent display under program control. Each auxiliary scope is mounted in a lighttight cabinet and is viewed by a high-resolution TV camera. To generate a color display, each of the three scopes was assigned a primary color - red, green, and blue. The three TV cameras were driven by a common synchronous generator and the camera signals were fed to a standard RGB (red, green, blue) color monitor. By using the three primary colors in a binary mode, seven basic colors (in addition to black) could be immediately obtained: red, green, blue, yellow (red and green), cyan (green and blue), magenta (red and blue), and white (red, green, and blue). By varying the intensity level of each primary color independently, a very large number of colors could be produced. Initially, the number of display colors was limited to 28 (plus black). They were the seven basic colors with four intensities each. More than four intensity levels could not be easily distinguished.

Both the intensity levels and the basic colors were controlled by program statements which turned the proper scopes on or off. To simplify usage,

a subroutine was written which would choose the basic color and intensity with a single statement in the user's program.

There were several substantial problem areas connected with color vector graphics. The four intensities of each basic color were very difficult to distinguish because the lines were very narrow usually with large space between them. Since it was impractical to vector-fill between every line to produce large areas of color, only the highest intensity on each basic color could be used; thus the number of colors available for display was reduced to seven (plus black).

Another problem related to producing a color vector display using the Adage system concerned the precise registration of the three images. The three scopes and camera systems had to be aligned so that images from each scope were superimposed exactly on the TV screen. To produce yellow, for example, the red image had to overlay the green image; otherwise, red and green fringes would appear. The scopes and camera also had to be adjusted for brightness, gain, blanking level, etc., to match the signals from each camera. Only by making careful mechanical and electrical adjustments of the cameras and scopes was it possible to produce an acceptable display.

A method of obtaining color hardcopies from the Adage system in the form of photographs, either Polaroid or conventional, was designed to accompany the color display system. A camera was mounted in a lighttight box in front of a fourth scope. A motor-driven filter wheel containing a segment of red, green, and blue filter was located in front of the camera lens. A cam and switch arrangement mounted on the color wheel switched one of the three displays to this scope as the appropriate filter passed by the camera lens. The wheel made one revolution and stopped automatically. It took approximately 1 minute to complete the exposure. Since the picture was taken from a single scope and the TV link was bypassed, all registration and alignment problems were eliminated.

Color Raster Graphics

With experience, it became increasingly clear that the best way to represent the variation of a scalar parameter on the surface of a three-dimensional object was by color-coding the parameter and displaying the solid object (with hidden surfaces removed) on a color raster graphics display device. Fortunately a digital color TV display system, which was being developed primarily to support image processing applications, was available. Consequently, the decision was made to halt the research and development effort based on the Adage display system and concentrate instead on the use of this digital raster display system.

The development of raster display hardware began with a disk-based system. This original system had a resolution of 480 lines with 640 picture elements (pixels) per line. There was a 3-bit data word per pixel, each bit in the data word being assigned to a primary color (red, green, and blue). The output device was an RGB color TV monitor. With this system it was possible to produce a picture in raster mode with entire surface panels, rather than

just the perimeter of the panels, colored. The picture could contain up to seven colors (plus black).

The disk-based system was later expanded to 6 bits per pixel to accommodate additional colors. At the same time a color control unit was placed into operation. This unit allowed a user to select from a table of 512 colors generated by setting each of the RGB primaries independently to 1 of 8 intensity levels. The 6-bit pixel value served then as an address into a 64-element color table which was determined by the user.

On the basis of the experience gained by using the Adage and the disk-based display systems, new display hardware was designed and implemented to provide greater flexibility and support for color graphics users. This new hardware consists of a new raster display unit (RDU) and an off-line microprocessor-based display system. This equipment forms the current version of the digital raster display system (fig. 5).

The new RDU replaced the disk-based system. It was designed to take advantage of new integrated circuit memory technology to replace the electromechanical disk memory. The RDU consists of two input data ports, a 2×10^6 bit solid-state memory, and control and timing logic for driving color TV monitors. One input port is connected directly to a data channel of the CDC 6600 computer, and the other is connected to the off-line system discussed later. Thus, the RDU can display data in an on-line mode and in an off-line mode. The image format is 480 lines with 640 pixels per line and 6 bits per pixel, and is compatible with standard 525-line TV monitors.

The initial goal was to establish an off-line system to support color graphics users as well as image processing applications. Many digital imagery calculations and some raster graphic calculations are time consuming because of the number of data points that must be computed; thus, in many cases it is impractical to submit a job and wait for the results in real time. An off-line system permits the saved image files to be displayed at the user's convenience. An off-line system also permits color hardcopy equipment such as film writers to be interfaced without developing large computer system software to drive them.

To satisfy this requirement, an off-line system was designed and implemented. This is a microprocessor-based system capable of displaying and making hardcopies of digital imagery and raster graphic data. The equipment consists of a nine-track dual-density magnetic tape drive, a microprocessor controller, a color film writer, and a CRT terminal. The system display device is the RDU.

The heart of the off-line system is an INTEL system 80/20-4 microprocessor. This is an 8-bit microcomputer capable of executing 76 instructions with an instruction execution time of 2 to 5 microseconds. It is a versatile machine, particularly suited for data handling with its programmable input/output ports. The microprocessor system was tailored for this application with three printed circuit boards - the central processing unit (CPU), a memory expansion board, and a direct memory access (DMA) controller. This configuration gave the system a capacity of 12 000 words (8 bit) of read-only memory (ROM) and 12 000 words

of random access memory (RAM), twelve 8-bit parallel input/output ports, two serial data ports, and a high-speed DMA port. The ROM is used for program storage (firmware) while the RAM is used as a tape data buffer and temporary data locations for program execution. The parallel ports are interfaced with the tape drive, film writer, and RDU. The DMA port is connected to the tape drive to handle the high data transfer rate.

All system activity is controlled by the microprocessor through commands entered at the CRT terminal. The system software interprets character commands entered by a user to perform the desired function. Since the system was expected to be used by a variety of users, the command syntax was designed to simplify system operation. The system commands fall into several broad areas. A group of commands are used for tape manipulations including commands to skip or backspace files or records. Other commands allow generation of test patterns on the TV display or film writer and loading and manipulating color tables. A third group of commands controls the displaying or recording of an image on the TV or film writer, respectively. These commands utilize additional parameters input by the user to control display size and content. They cause the data to be read from the magnetic tape and output to the RDU or film writer. The system currently accepts 35 commands and the system firmware occupies approximately 5000 words of ROM. The system has expanded color capability; that is, the color table was enlarged to allow each primary color to be displayed with 64 intensity levels. Thus, a user can choose from a table of 2^{18} possible colors.

The film writer interfaced with the system has 2048 pixel by 2048 line resolution with 256 intensity levels per color. It will record images on Polaroid film, sheet film, and 35-mm film.

COLOR GRAPHICS METHODOLOGY

Color graphic representations of the vehicle surface were employed to investigate both heat-sink material thicknesses and surface temperatures. Displays of the skin thickness are discussed in this section to describe in more detail the color graphics methodology. The two color patterns chosen to represent the skin thicknesses are shown in figure 6. Black was always the background color; 7 colors represented the surface values in the first pattern and 15 colors represented surface values in the second. Each color was chosen to represent the small band of thicknesses shown in the key. All figures containing color representations of thickness can be interpreted according to this key. The progressive color theme was an arbitrary aesthetic choice which was intended to coordinate hottest to coolest (white to blue) colors with maximum to minimum values.

The two color graphics approaches (vector and raster) which were investigated are illustrated in figure 7. These individual pictures are reproductions of Polaroid shots of the screen displays which were the standard permanent record mode for this study. Several new geometry enhancement routines were required in both the vector and raster graphics software to achieve satisfactory displays. The initial routine coded for the Adage display terminal to plot the boundary lines of the individual panels with a user-specified

color-thickness schedule resulted in the geometry display shown in figure 7(a). The problem with this approach is that a single line is generally a common boundary between two panels which often require different colors. Different colors plotted in the same spatial location cannot be identified and tend to be displayed as white. To alleviate this problem, a routine to locally shrink each panel about its centroid in an average plane defined by its corner points was added to the basic geometry package. The degree of shrinking was a user-controlled option, and through a short trial and error session, the vector representation illustrated in figure 7(b) was produced. The trial and error approach can easily be eliminated by making the degree of shrinking a function of numerical model scale. More important, however, is the fact that the colors of the individual panels (and therefore the local thicknesses) are recognizable.

The routine developed for the digital raster display system presented a slightly different geometry problem. The display image is generated panel by panel in the order of original geometry definition and all pixels inside the panel boundaries are assigned a specific color. Unfortunately, the original geometry definition was incompatible with a straightforward application of this technique. Since there was no component shielding capability, the color pattern within the total geometry outline depended primarily on the order in which the panels were considered. In the geometry scheme used here, the order of geometry components was fuselage, wing, and vertical tail, so that in a raster image of the vehicle view in the right side of figure 7(b), the complete vertical tail would be visible when in fact it should be partially hidden behind the wing. A simple hidden surface routine was developed and employed to generate the results shown in figure 7(c). The technique was to calculate a depth dimension of each panel centroid in the rotated view in addition to its lateral and vertical position already being calculated. In this manner, each element that appeared in the vector drawings could be plotted as usual with colors of only panels closest to the viewer replacing any previous colors. This technique is very rapid and effective when the panel sizes are small, as illustrated in the right side of figure 7(c) by the vertical tail cut off by the wing leading edge. When large panels are employed, geometry irregularities are generated, such as the intersection of the vertical tail with the fuselage illustrated in the left side of figure 7(c). More comprehensive hidden surface routines would eliminate this problem. Figure 7(c) was generated using 7 colors (plus the background), while the same data using 15 colors (plus the background) are illustrated in figure 7(e). As expected, the detail of skin-thickness-distribution patterns is enhanced with application of more colors (smaller thickness ranges associated with each color). The number of colors required depends of course on the research application and tends to vary between researchers.

DESIGN APPLICATION

Skin-Thickness Distributions

A comparison between the vehicle heat loads for the maximum Mach number dash capability (M_{max} = 8.8) and for the cruise capability at Mach 6 was presented in figure 4. These heat-load histories represent two Lockalloy heat-sink skins (one for each mission), where each panel thickness was sized so that its maximum surface temperature would exactly reach but not exceed a

value of 589 K during the particular mission under investigation. A color representation of the skin-thickness distribution for the maximum Mach number dash mission is presented in figure 7(c), and the skin-thickness distribution for 120 sec of cruise at Mach 6 mission is presented in figure 7(d). Increased thickness corresponds to increased total heat load. The close similarity between the two color patterns indicates that a thermal protection scheme established for the dash mission should be effective for the cruise mission (or vice versa if 120 sec of cruise controlled the design). More complete compatibility may result if the thickest elements from each design requirement are combined into a single thickness matrix. The thickness-distribution displays highlight one potentially major design problem in the region of the canopy. The canopy is subjected to the same total heat loads as the fuselage nose and component leading edges; therefore, the requirements for pilot visibility could pose a severe local design challenge. As stated earlier, a rapid means of identifying potential problems was the research goal for this study.

Surface Temperatures

Color-coded plots of the vehicle geometry at specific instants during the mission can also be used to represent the surface-temperature histories. A color image of the absolute surface temperatures can easily be created by dividing the expected overall temperature rise by the number of colors desired to define a temperature range for each shade. This is an effective means for quickly identifying points in the trajectory where any average vehicle temperature occurs; however, this type information is not very difficult to obtain from numerical printouts. The temperature history of the vehicle for the maximum Mach number dash trajectory (shown in fig. 3(a)) is presented in figure 8. Zero time is set when the vehicle reaches Mach 2 during ascent, where the transient heating calculations were initiated. The vehicle was assumed to be at a uniform initial temperature of 256 K (0° F). A maximum allowable temperature (T_{limit}) for Lockalloy was held constant at 589 K indicated by the pointer on the ordinate. Time traces of the maximum, minimum, and area-weighted average surface temperatures are presented. Note that the maximum Mach number of 8.8 occurs 90 sec after Mach 2, while the maximum temperature rise does not occur until well into the descent at $t - t_i = 240$ sec, where the Mach number is 4.5. The objective of this application of color graphics was to develop a means of rapidly identifying regions of thermal gradients where potentially large thermal stresses might occur. The limits of possible gradients are defined by the difference between the maximum and minimum temperatures occurring on the vehicle surface at any instant in time, as shown at the top of figure 8. Since the maximum potential ($T_{max} - T_{min}$) for thermal gradients tends to be much less than the overall vehicle temperature rise ($T_{limit} - T_i$), color displays of surface temperatures within the local $T_{max} - T_{min}$ boundaries can be used more effectively to identify gradients with as few as seven colors (plus background). This technique was employed in the following manner. The area-weighted average temperature for the vehicle was calculated at each trajectory point of interest. Red was always used to designate a small temperature range around the vehicle average. Yellows and whites were used to designate temperatures above the average, while all other colors represented temperatures below the average, as indicated by the two color temperature keys in figure 9. These two keys, fig-

ure 9(a) for the 7-color matrix and figure 9(b) for the 15-color matrix, apply for all subsequent temperature histories.

The sequence of photographs shown in figure 10 is a color vector graphics representation of the surface-temperature gradients for the maximum Mach number dash mission (figs. 3(a) and 8) using the skin thicknesses calculated for that specific mission. Figure 10(a) is presented to identify the image that appears when the temperature differences are less than ±5 K from the average (i.e., essentially no thermal gradient present). The overall temperature characteristics illustrated in figure 10 are nearly self-explanatory. Temperatures on the thinnest panels on the upper surface of the vehicle and the boattail region to the rear of the fuselage rise more rapidly than the thicker panels, even though both types reach the identical maximum temperature during the mission. This characteristic is primarily due to surface radiation which is much more effective in reducing total heat load in those regions where convective heating is low. This radiation effect is amplified when materials with higher limiting temperatures are employed (ref. 4).

The examination criterion for spotting areas of potential thermal stress is to identify individual panels (or small groups of panels) of one color which are bounded by panels of a different color. Figure 10(c) presents two examples that occur during ascent. The canopy area is cooler than its surroundings, while a white rearward panel on the side of the upper surface between the wing and the vertical tail is hotter than it surroundings. This panel exhibits the same trend in figures 10(d) and 10(e). In figures 10(f), 10(g), and 10(h), the temperature of a few panels on the upper fuselage behind the canopy lags a little behind the temperature of their surroundings. Also in figure 10(h), the temperature of the chines along the lower portion of the fuselage appears elevated above that of their surroundings. The temperature gradients are rather small as the maximum allowable temperature (T_{limit} = 589 K) of the material is approached, as indicated by figures 10(i) through 10(ℓ).

The temperature differences over the vehicle increase rapidly during the last stages of descent for which heating calculations were made. The maximum values occur at the last calculation point (fig. 11(o)), as indicated by the presence of all seven available colors (white through blue). The temperature differences, however, are primarily between the upper and lower surfaces of the vehicle and are fairly regular from nose to tail rather than a series of local hot spots. This trend would cause a general bending upward of the nose and tail (or leading and trailing edges) which must be accommodated in the primary structure.

Before any final evaluation of the structure and TPS is undertaken, an examination of off-design heating is warranted to obtain a general definition of thermal gradient patterns and possible regions of design emphasis. Off-design heating is defined here simply as the transient heating for any given skin-thickness distribution over a set of flight conditions (or vehicle trajectory) other than those used to initially size the panel thicknesses. For example, calculating the heating over a trajectory for 120 sec of cruise at Mach 6 on a skin-thickness distribution sized precisely to meet the TPS requirements for a Mach 8.8 dash trajectory is considered off-design heating analysis. The overall vehicle surface-temperature history for 60 sec of cruise

at Mach 6 mission using the skin thicknesses prescribed for the maximum Mach number dash mission is presented in figure 11. The total heat load for the 60 sec of cruise mission is much less than that for the dash mission (fig. 4). In fact, the maximum value of average vehicle surface temperature is 60 K less than the maximum allowable temperature, as shown in the lower portion of figure 11, even though some panels do come within 10 K of the limiting temperature, as indicated by the vehicle maximum temperature curve. The potential for thermal gradients, however, is not reduced, as indicated by the upper portion of figure 11. Also, the maximum potential does not occur at the end of descent calculations, but much earlier at approximately 200 sec after Mach 2 in ascent ($t - t_i = 200$ sec).

An abbreviated color raster graphics display of the temperature history for this mission is presented in figure 12. Figure 12(a) is presented as a reference raster image that would appear in the absence of any thermal gradients. The raster images allow easier identification of panels with elevated temperatures such as that on the side of the upper fuselage between the wing and vertical tail in figure 12(b). This same panel was identified in the vector graphics representation of the temperature history for the maximum Mach number dash mission (fig. 10(c)) and can be used as a comparison. Also, smaller local gradient regions common to both missions such as the white streak along the rear of the lower fuselage chine shown in the right images of figures 12(b) and 12(e) are clearly distinguishable in raster images but not in vector images (figs. 10(c) through 10(h)). These areas, as well as less obvious gradients (such as those along the wing leading edge), are even more identifiable from the full screen image rather than the reduced Polaroid reproductions in figure 12. The reproduction of the right side of figure 12(d) presented in figure 13 has a raster image size closer to that which would appear on screen. The annotation and color key shown in figure 13 were not generally employed during the conceptual design cycle. They are presented here to illustrate some of the versatility available in the color graphics scheme, particularly for generating fairly complete and detailed figures for any given data set.

Further examination of the temperature history of the skin thicknesses for the maximum Mach number dash mission during the 60 sec of cruise at Mach 6 mission reveals some new local temperature gradient patterns which could affect overall TPS design. The local hot spots indicated near the middle of the upper fuselage (figs. 12(c) and 12(d)) are related to very thin panels and may require relief from compression loads. The heating irregularity occurring in the small region on the side near midfuselage, illustrated in figures 12(d) through 12(g), is the result of a TPS requirement for slightly thicker panels. Some additional irregular heating occurs in the canopy region of the upper fuselage (visible in the left side of fig. 12(f)) and may also require further design refinement. The remainder of the temperature differences shown in figure 12(f) are fairly regular and are consistent with the overall vehicle TPS design requirements previously identified from figures 10(m) through 10(o).

The total heat loads for the maximum Mach number dash mission and the 120 sec of cruise at Mach 6 mission were nearly identical when design skin-thickness distributions for each mission were employed (fig. 4). The heating distribution, however, is not equivalent, as indicated by the overall vehicle surface-temperature history presented in figure 14 for the dash mission skin

thicknesses during the 120 sec of cruise mission. The average vehicle temperature slightly exceeds the maximum allowable temperature for a brief period at a $t - t_i$ of approximately 300 sec. The maximum vehicle surface temperature indicates that some panels exceed the temperature limit for approximately 180 sec (200 sec < $t - t_i$ < 380 sec). The overall potential for thermal gradients, however, is no greater than for any other mission requirement as shown in the upper portion of figure 14.

A color raster graphics representation of the surface-temperature gradients is presented in figure 15. The gradients during ascent and the first 60 sec of cruise of this mission are identical to those previously shown in figure 12; therefore, the first image is at 143 sec, just beyond midcruise. The irregular heating pattern occurring near midfuselage is slightly exaggerated, as shown in figure 15(c); however, the temperature gradients in later stages of the mission are less than those encountered during the maximum Mach number dash mission used to size the skin thicknesses. Since the average temperatures related to figures 15(c) and 15(d) are very nearly equal to the limiting temperature, all yellow and white panels in these two figures need to be thickened slightly to accommodate both the 120 sec of cruise at Mach 6 mission and the maximum Mach number dash mission.

The temperature histories and the skin-thickness distributions for the two missions were numerically searched to establish a new thickness distribution adequate for both missions. Total vehicle weight did not increase enough to significantly alter the maximum performance trajectories already established. Therefore, the temperature histories resulting from the new thickness distribution were calculated over the same mission and flight conditions displayed in figure 3. The history of the extremes ($T_{max} - T_{min}$) and average vehicle surface temperature for the maximum Mach number dash mission is presented in figure 16. None of the panels exceed the maximum allowable temperature, and the maximum potential for thermal gradients at the end of heating calculations is approximately the same as that for the original skin thicknesses (fig. 8). The temperature differences during earlier portions of the trajectory are somewhat amplified, particularly during descent ($t - t_i$ greater than 90 sec).

Raster graphics images (with 15-color matrix) representing the surface-temperature histories of each panel are contained in figure 17. The temperature histories of each panel are contained in figure 17. The temperature gradients through 90 sec (figs. 17(a) and 17(b)) are quite regular. From that point on (figs. 17(c) through 17(e)), the irregular pattern near midfuselage previously exhibited during cruise is now evident during the dash mission as well. In addition, an irregularity on the upper surface of the wing and on the forward portion of the lower fuselage (fig. 17(c)) results from local thickening of the skin.

The temperature history during the 120 sec of cruise at Mach 6 mission has undergone a more radical change, as shown in figure 18. The maximum surface temperature of the new set of skin thicknesses just reaches but does not exceed the limit. In addition, by comparing the upper portions of figures 18 and 14, the potential for thermal gradients is seen to be less than previously encountered throughout the flight trajectory. This trend is also evident in the

15-color raster graphics images of this temperature history presented in figure 19. The temperature patterns are much more regular over the entire trajectory. A few irregularities still persist. The panel at the rear of the upper fuselage between the wing and vertical tail continues to maintain an elevated temperature compared with its surroundings during ascent and cruise (figs. 19(a), 19(b), and 19(c)), while this trend reverses during descent (figs. 19(d) and 19(e)). The panels located on the upper center line near midfuselage are also at elevated temperatures through cruise (figs. 19(a) through 19(c)). A slight gradient in the region of chines on the lower fuselage is also evident throughout the trajectory, and a momentary hot spot appears in the upper surface of the wing during descent (fig. 19(d)).

The overall significance of the thermal gradients illustrated in this paper in constraining the structure and heat-sink TPS design is not easy to determine. It would probably be obvious to most structural analysts that any thermal stresses resulting from the typical gradients shown (less than 50 K between adjacent panels at working temperatures less than 600 K) would be well within the yield strength of Lockalloy for any reasonable structural design. Since this color application methodology was developed during the research airplane design study, Lockalloy skin thicknesses and temperature histories were used exclusively in order to maximize the immediate design benefit resulting from color graphics.

As stated earlier, three other candidate materials - aluminum, titanium, and beryllium - as well as combinations of these materials in conjunction with Lockalloy were also investigated, although primarily from the standpoint of vehicle dry weight versus performance, as reported in reference 4. The application of color graphics may have had more impact on the TPS design in the analysis of titanium or beryllium because of the increase in magnitude of surface-temperature differences with these materials. A comparative example of the potential gradients for each of the four materials is shown in figure 20. The transient heating was calculated for a dash mission at the maximum Mach number achievable with the minimum TPS weight for each material. These Mach numbers and the maximum allowable temperature for each material are presented in the figure. The lower maximum Mach number for Lockalloy (8.4 rather than 8.8) is due to a minimum skin-thickness constraint of 0.914 cm (0.090 in.) imposed because of pressure loads and secondary trajectory iterations to optimize average thicknesses. Similar constraints were imposed on the other materials, so that the comparisons are valid. The potential for thermal gradients ($T_{max} - T_{min}$) of titanium is more than three times that for Lockalloy over most of their respective trajectories. Beryllium temperature ranges are generally more than five times those for Lockalloy. This potential for thermal gradients is not any assessment of the real value of these materials for a heat-sink TPS but is presented here merely to illustrate the possible advantages of color graphics in a more comprehensive design and evaluation cycle.

CONCLUDING REMARKS

Color images of skin thicknesses and surface-temperature gradients are a powerful aid in quickly sorting through the mass of aerothermodynamic infor-

mation that must be generated and evaluated to support design of a heat-sink thermal protection system. Areas of high heating and thermal patterns which could result in subsequent structural design problems can be identified quickly in order to minimize the design effort. Although raster graphic displays are generally superior, since they provide a solid object representation rather than a wire frame representation, the creation of either vector or raster color images representing physical quantities on the surface of a given vehicle is straightforward and relatively simple. This is particularly true when the magnitudes of the physical quantities represented by various colors tend to be uniform over discrete areas of the vehicle. Paneling methods, such as those used here for transient heating analysis, tend to be a mainstay in conceptual design for most of the disciplines and are ideally suited for color application. Color images of other parameters such as pressures, normal forces and loads, moments, and all aerodynamic coefficients could also be displayed and evaluated very effectively during conceptual design provided that their values are known for each panel.

Langley Research Center
National Aeronautics and Space Administration
Hampton, VA 23665
May 22, 1979

REFERENCES

1. Kirkham, F. S.; Jones, R. A.; Buck, M. L.; and Zima, W. P.: Joint USAF/NASA Hypersonic Research Aircraft Study. AIAA Paper No. 75-1039, Aug. 1975.

2. Combs, H. G.; et al.: Configuration Development Study of the X-24C Hypersonic Research Airplane - Executive Summary. NASA CR-145274, 1977.

3. Jackson, L. Robert; and Taylor, Allan H.: A Structural Design for a Hypersonic Research Aircraft. AIAA Paper No. 76-906, Sept. 1976.

4. Vahl, W. A.; and Edwards, C. L. W.: Study of Heat Sink Thermal Protection Systems for Hypersonic Research Aircraft. AIAA Paper 78-38, Jan. 1978.

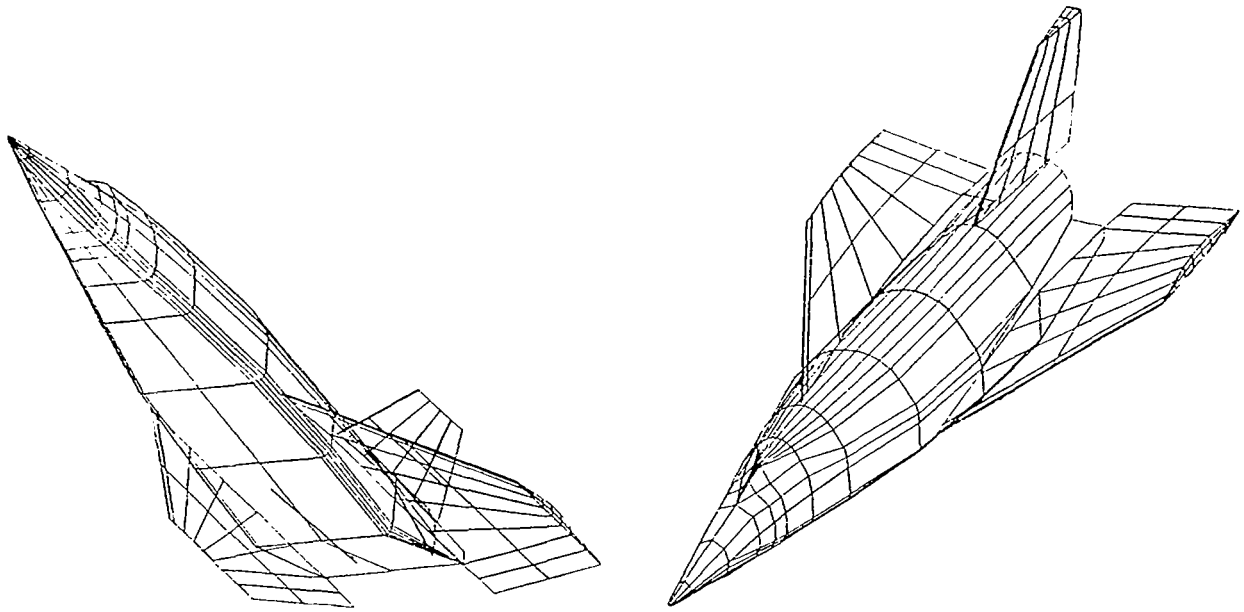

Figure 1.- Surface panel distribution used to make heating calculations and size the heat-sink TPS. 200 surface panels employed.

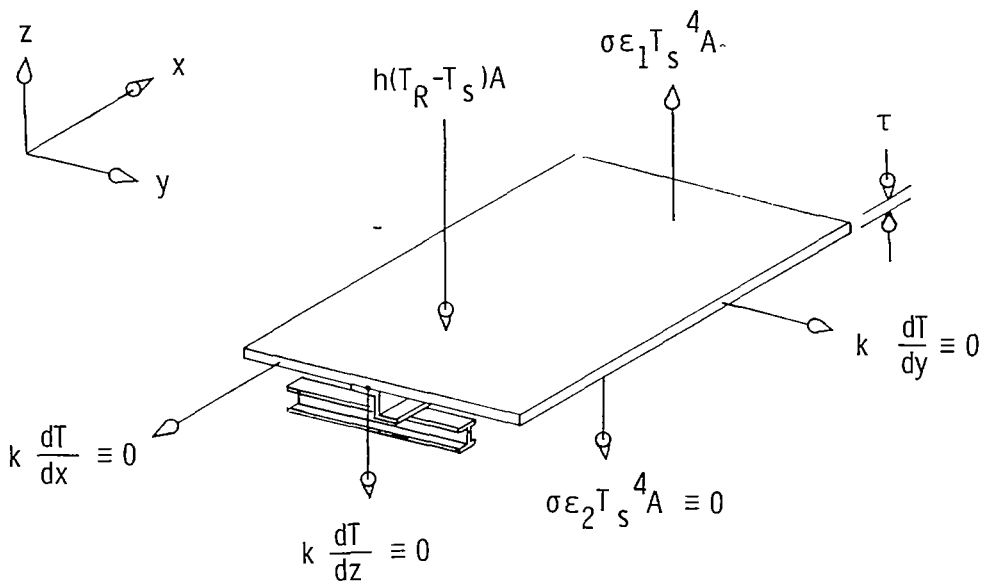

Figure 2.- Heat flow model assumed for each surface panel.

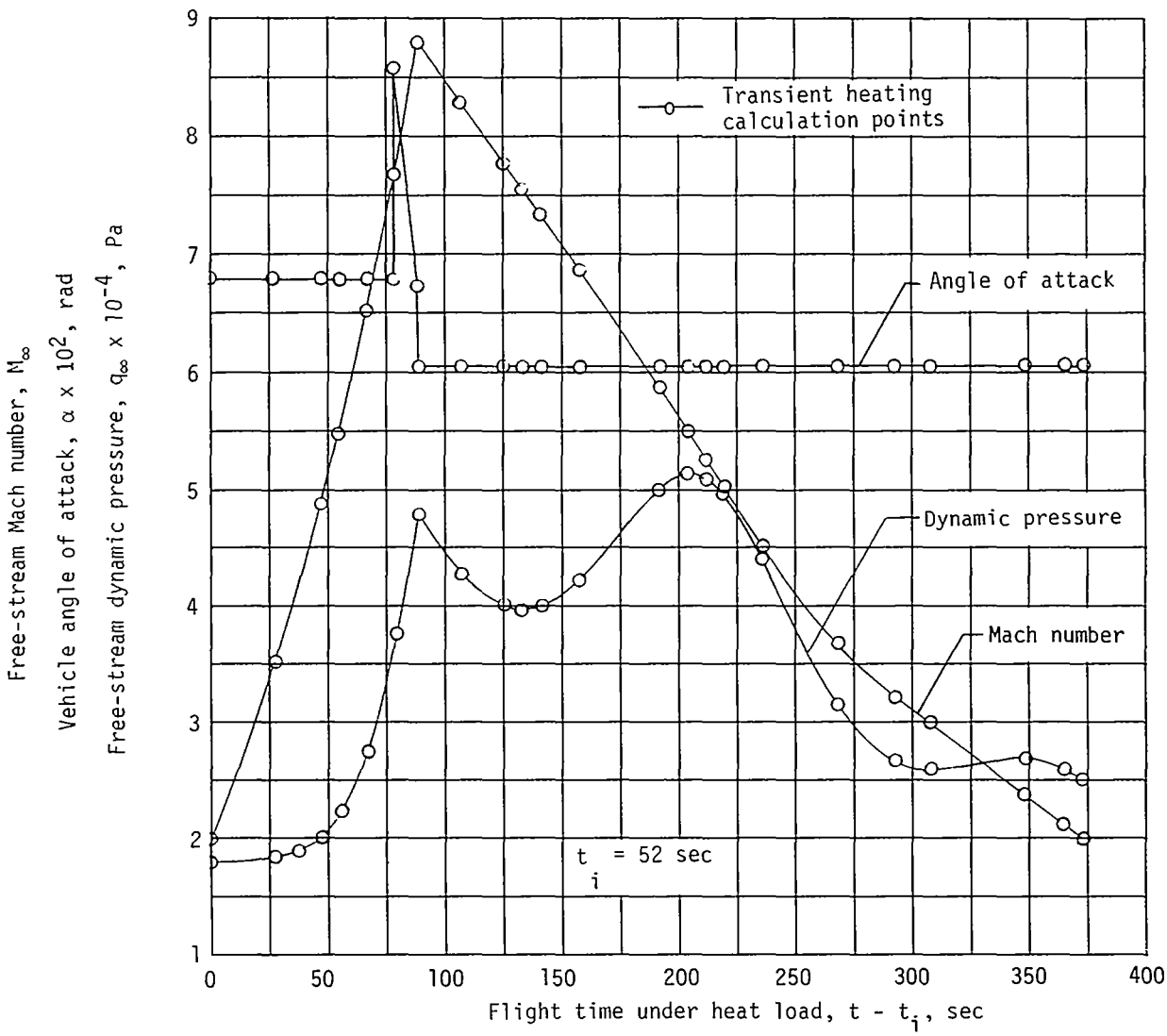

(a) Maximum Mach number dash mission.

Figure 3.- Typical flight conditions governing aerodynamic heating during two design-limiting missions using weights consistent with Lockalloy heat-sink TPS.

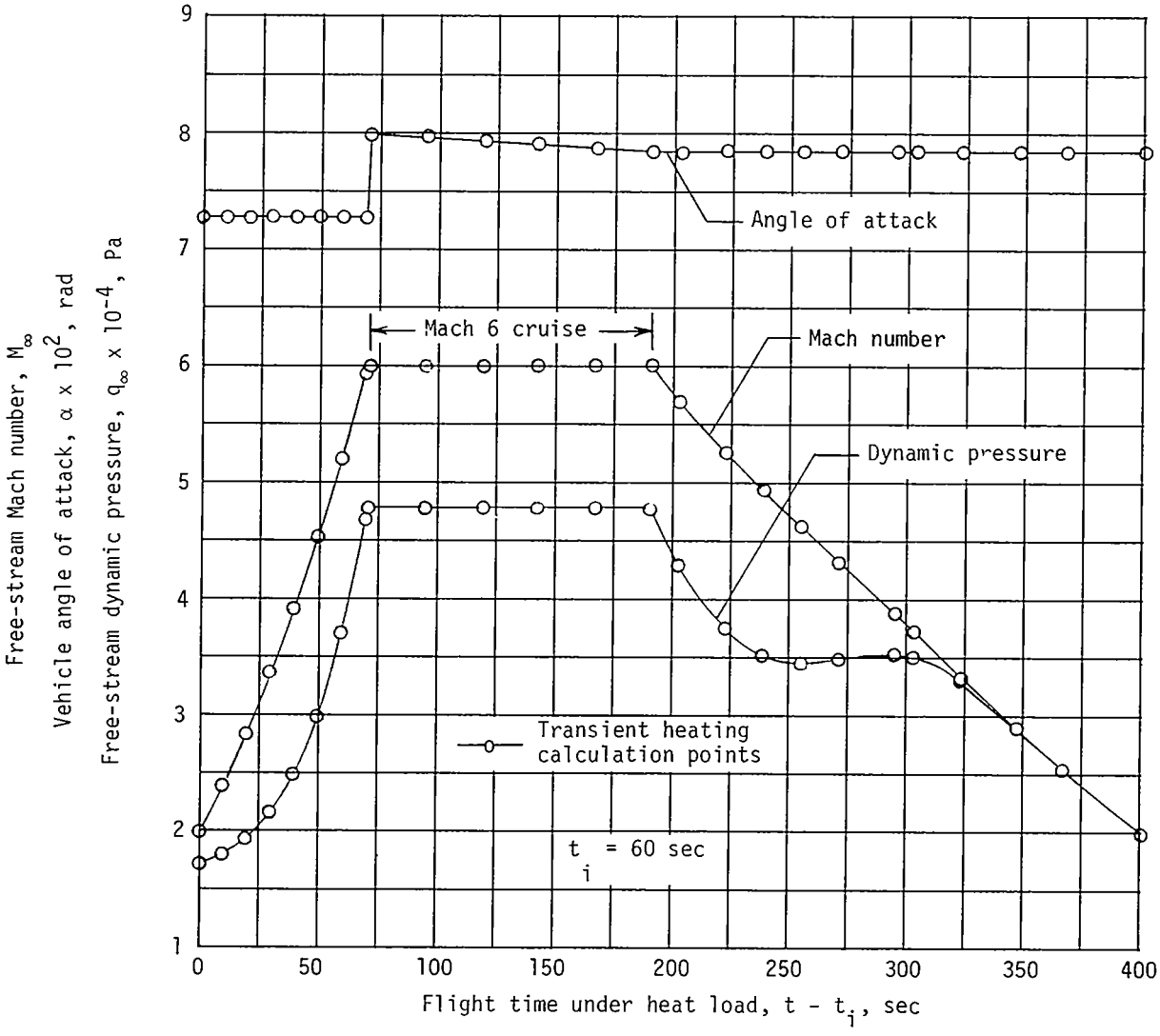

(b) 120 sec of cruise at Mach 6 mission.

Figure 3.- Concluded.

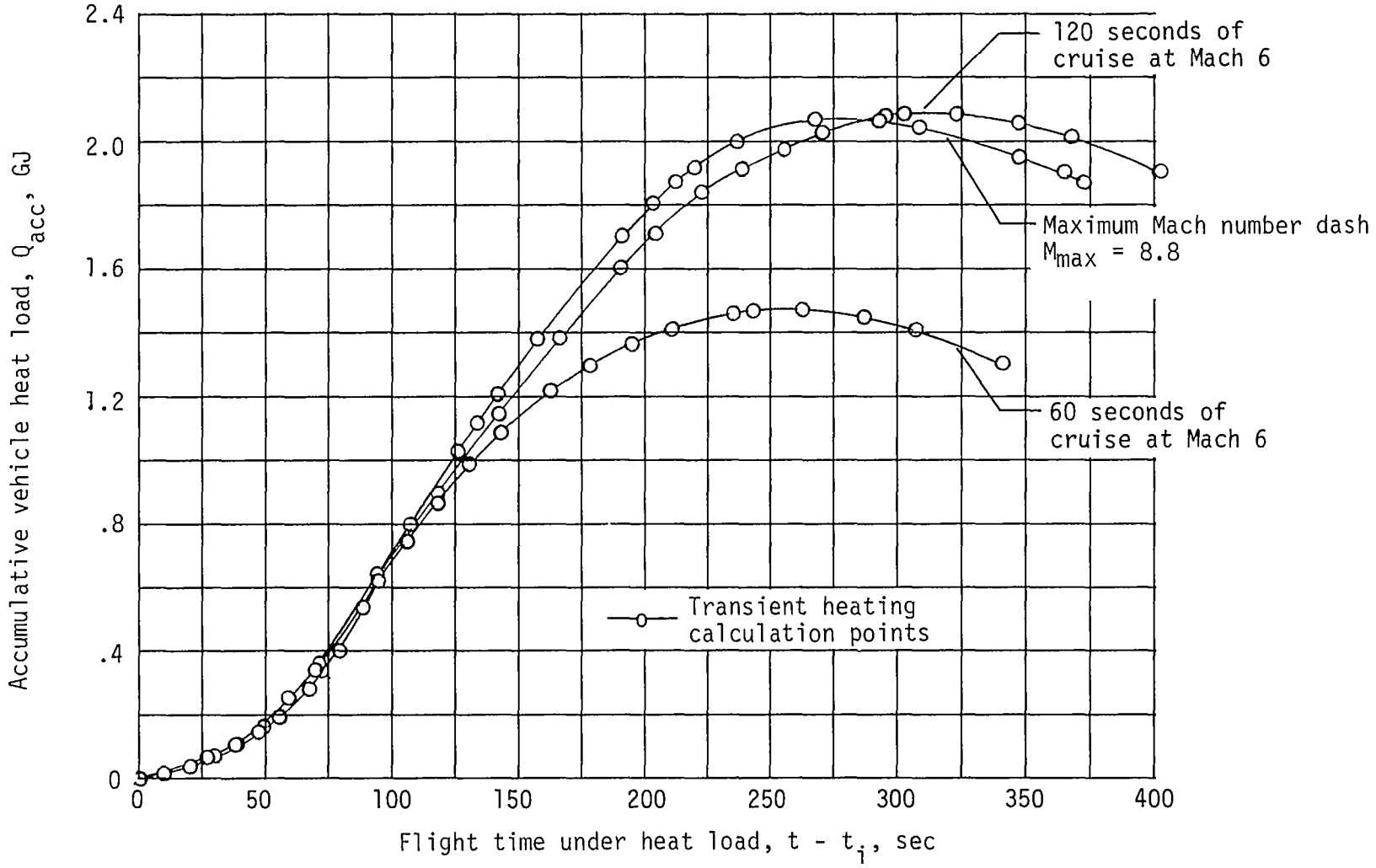

Figure 4.- Comparative heat loads to Lockalloy heat-sink thermal protection systems designed to accommodate heating during maximum Mach number dash mission and Mach 6 cruise missions.

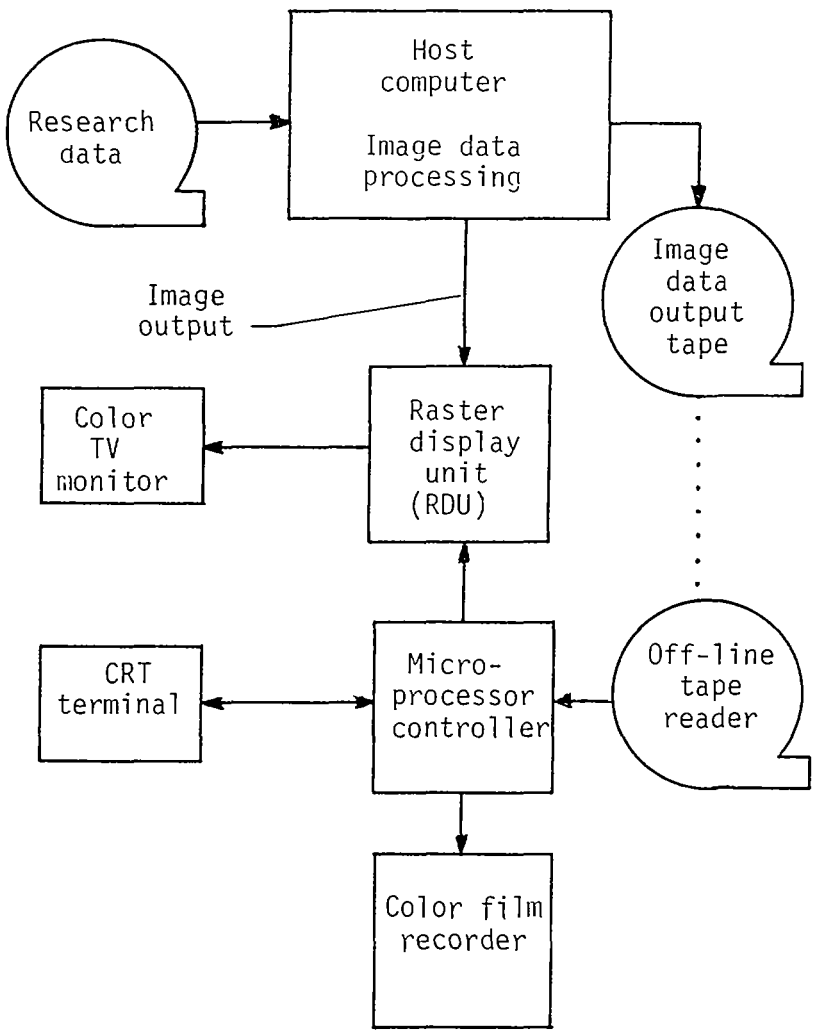

Figure 5.- Hardware configuration of digital raster display system.

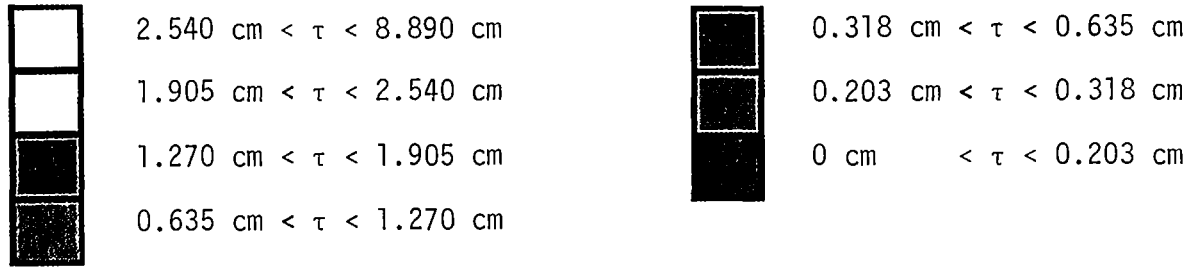

(a) With 7-color matrix.

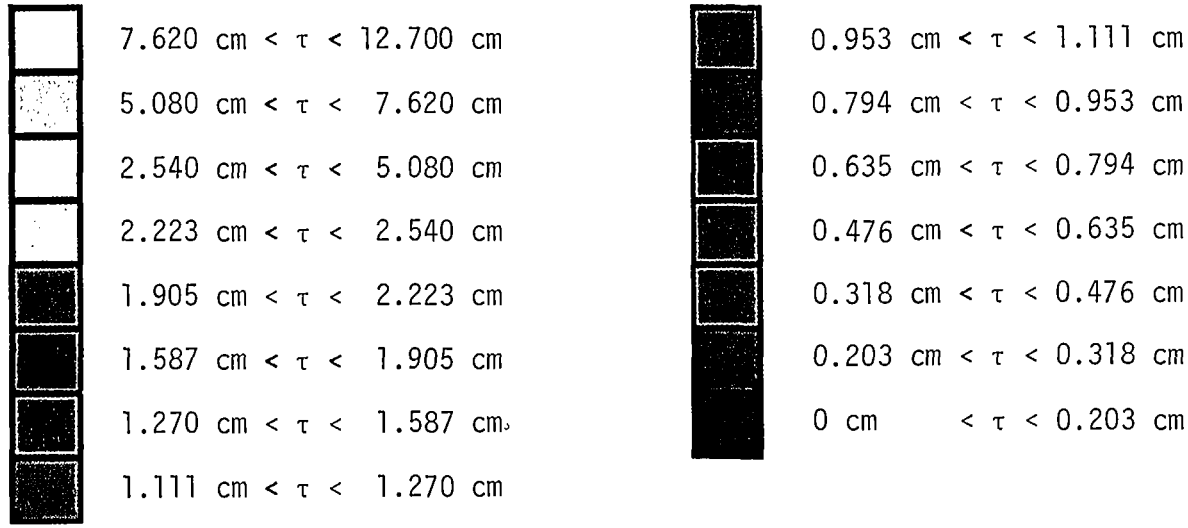

(b) With 15-color matrix.

L-79-166

Figure 6.- Correspondence between colors and skin thicknesses.

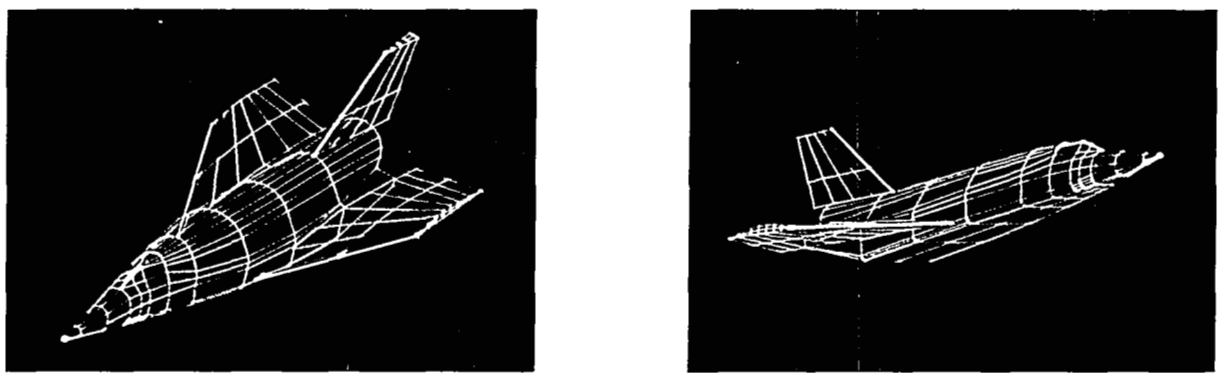

(a) 7-color vector graphics using full-size geometry panels.

(b) 7-color vector graphics using geometry panels locally reduced about their centroids. Maximum Mach number dash mission.

L-79-167

Figure 7.- Color-coded images illustrating skin-thickness distribution for Lockalloy heat-skin TPS on a hypersonic research airplane concept.

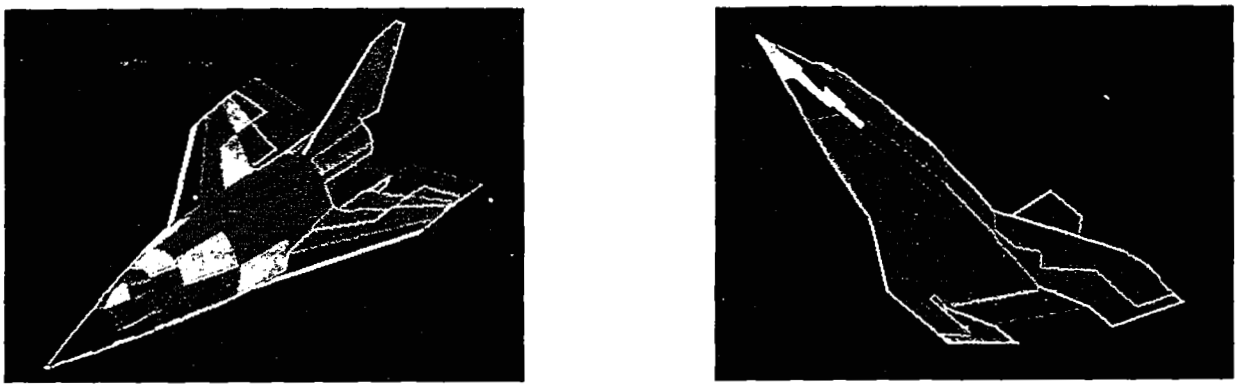

(c) 7-color raster graphics using full-size geometry panels and component shielding. Maximum Mach number dash mission.

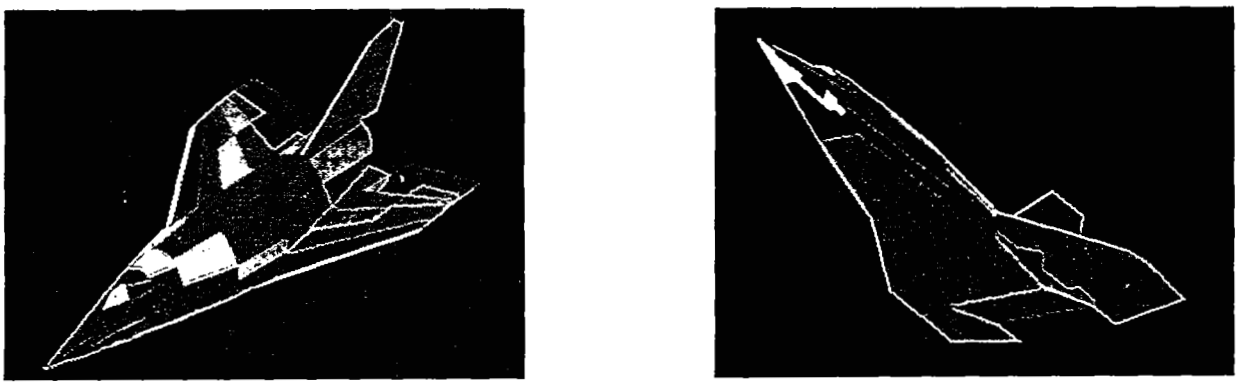

(d) 7-color raster graphics using full-size geometry panels and component shielding. 120 sec of cruise at Mach 6 mission.

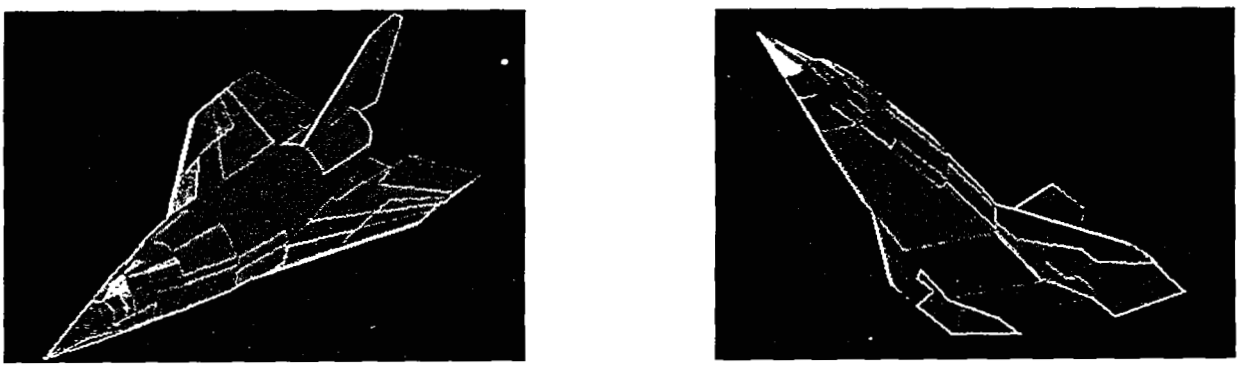

(e) 15-color raster graphics using full-size geometry panels and component shielding. Maximum Mach number dash mission.

L-79-168

Figure 7.- Concluded.

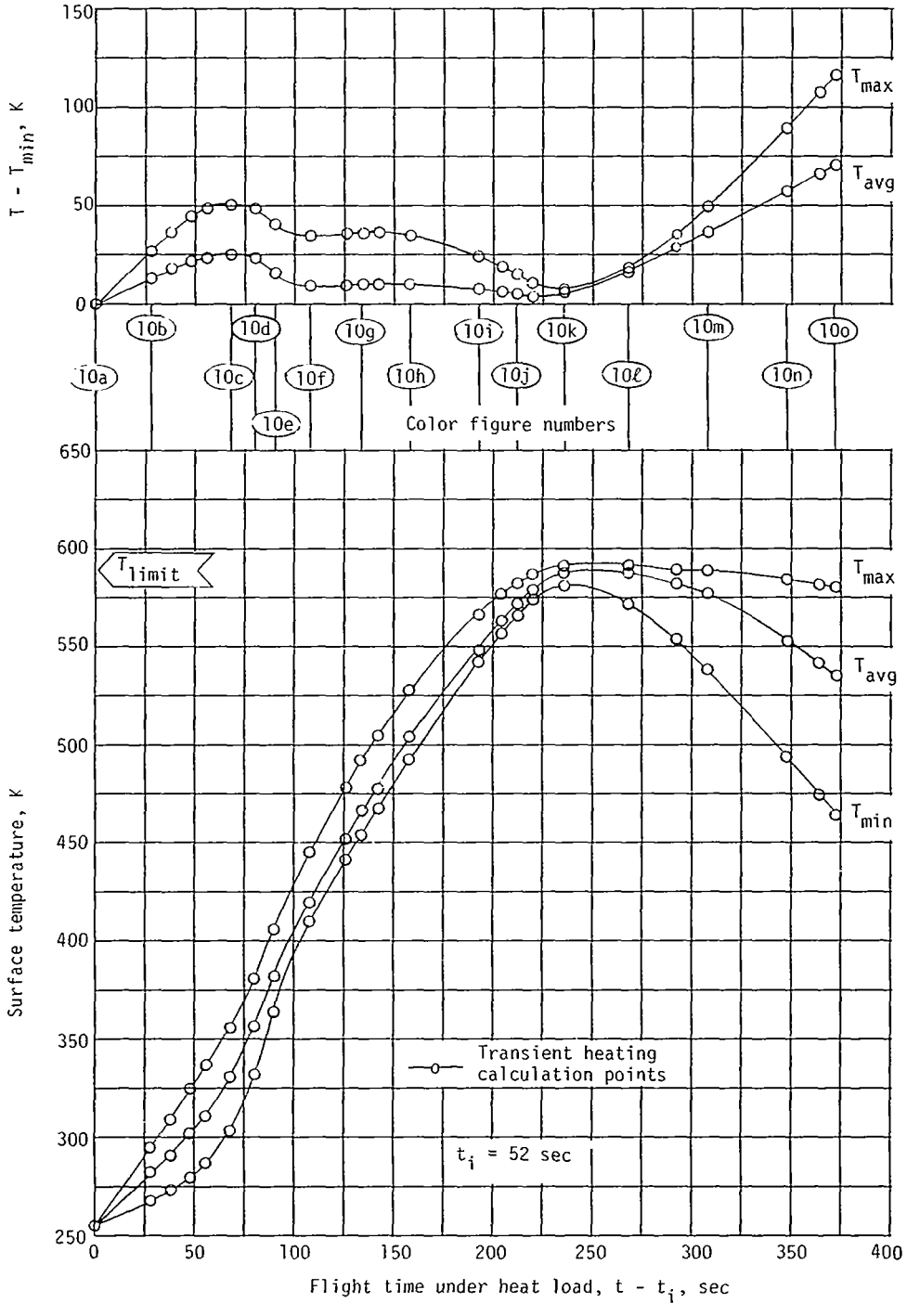

Figure 8.- Surface-temperature histories of on-design Lockalloy heat-sink TPS during maximum Mach number (M_{max} = 8.8) dash mission.

$20.0\ K < T_{loc} - T_{avg} < 35.0\ K$

$5.0\ K < T_{loc} - T_{avg} < 20.0\ K$

$-5.0\ K < T_{loc} - T_{avg} < 5.0\ K$

$-20.0\ K < T_{loc} - T_{avg} < -5.0\ K$

$-35.0\ K < T_{loc} - T_{avg} < -20.0\ K$

$-60.0\ K < T_{loc} - T_{avg} < -35.0\ K$

$-85.0\ K < T_{loc} - T_{avg} < -60.0\ K$

(a) With 7-color matrix.

$27.5\ K < T_{loc} - T_{avg} < 35.0\ K$

$20.0\ K < T_{loc} - T_{avg} < 27.5\ K$

$12.5\ K < T_{loc} - T_{avg} < 20.0\ K$

$5.0\ K < T_{loc} - T_{avg} < 12.5\ K$

$2.5\ K < T_{loc} - T_{avg} < 5.0\ K$

$-2.5\ K < T_{loc} - T_{avg} < 2.5\ K$

$-5.0\ K < T_{loc} - T_{avg} < -2.5\ K$

$-12.5\ K < T_{loc} - T_{avg} < -5.0\ K$

$-20.0\ K < T_{loc} - T_{avg} < -12.5\ K$

$-27.5\ K < T_{loc} - T_{avg} < -20.0\ K$

$-35.0\ K < T_{loc} - T_{avg} < -27.5\ K$

$-47.5\ K < T_{loc} - T_{avg} < -35.0\ K$

$-60.0\ K < T_{loc} - T_{avg} < -47.5\ K$

$-72.5\ K < T_{loc} - T_{avg} < -60.0\ K$

$-85.0\ K < T_{loc} - T_{avg} < -72.5\ K$

(b) With 15-color matrix.

L-79-169

Figure 9.- Correspondence between colors and surface temperatures.

(a) $t - t_i = 0$ sec; $M_\infty = 2.00$; $q_\infty = 18\ 099$ Pa; $\alpha = 0.0679$ rad;
$T_{max} = 255.6$ K; $T_{avg} = 255.6$ K; $T_{min} = 255.6$ K.

(b) $t - t_i = 28$ sec; $M_\infty = 3.50$; $q_\infty = 18\ 434$ Pa; $\alpha = 0.0679$ rad;
$T_{max} = 294.5$ K; $T_{avg} = 280.4$ K; $T_{min} = 266.8$ K.

(c) $t - t_i = 68$ sec; $M_\infty = 6.50$; $q_\infty = 27\ 771$ Pa; $\alpha = 0.0679$ rad;
$T_{max} = 355.8$ K; $T_{avg} = 331.0$ K; $T_{min} = 305.8$ K.

L-79-170

Figure 10.- Color-coded vector graphics images using 7-color matrix representing surface-temperature gradients of on-design Lockalloy heat-sink TPS during maximum Mach number ($M_{max} = 8.8$) dash mission.

(d) $t - t_i$ = 80 sec; M_∞ = 7.68; q_∞ = 37 107 Pa; α = 0.0854 rad;
T_{max} = 381.1 K; T_{avg} = 356.1 K; T_{min} = 332.5 K.

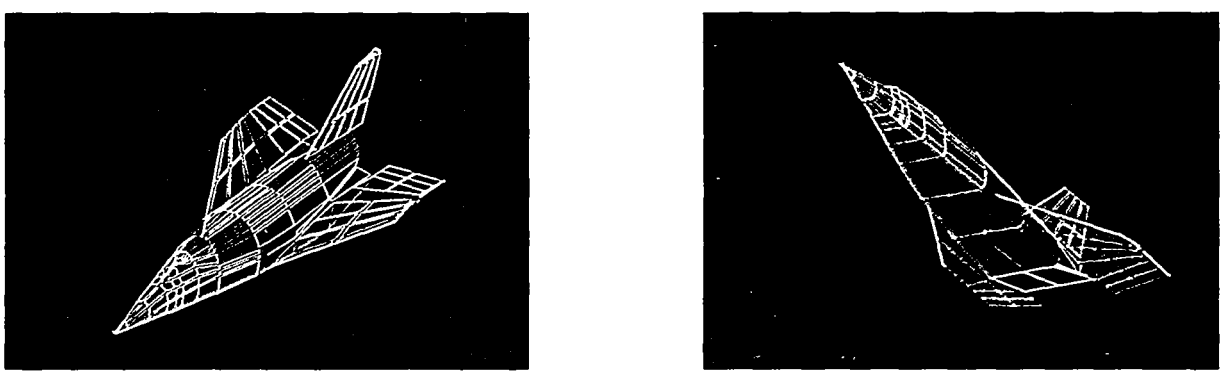

(e) $t - t_i$ = 90 sec; M_∞ = 8.78; q_∞ = 47 880 Pa; α = 0.0605 rad;
T_{max} = 405.4 K; T_{avg} = 381.5 K; T_{min} = 364.6 K.

(f) $t - t_i$ = 108 sec; M_∞ = 8.25; q_∞ = 42 709 Pa; α = 0.0605 rad;
T_{max} = 444.8 K; T_{avg} = 419.2 K; T_{min} = 409.7 K.

L-79-171

Figure 10.- Continued.

(g) $t - t_i$ = 134 sec; M_∞ = 7.55; q_∞ = 39 741 Pa; α = 0.0605 rad;
T_{max} = 491.6 K; T_{avg} = 465.5 K; T_{min} = 454.7 K.

(h) $t - t_i$ = 158 sec; M_∞ = 6.90; q_∞ = 42 278 Pa; α = 0.0605 rad;
T_{max} = 527.6 K; T_{avg} = 503.8 K; T_{min} = 492.8 K.

(i) $t - t_i$ = 192 sec; M_∞ = 5.92; q_∞ = 49 939 Pa; α = 0.0605 rad;
T_{max} = 565.5 K; T_{avg} = 549.4 K; T_{min} = 540.9 K.

L-79-172

Figure 10.- Continued.

(j) $t - t_i$ = 212 sec; M_∞ = 5.28; q_∞ = 51 088 Pa; α = 0.0605 rad;
T_{max} = 581.6 K; T_{avg} = 571.7 K; T_{min} = 565.3 K.

(k) $t - t_i$ = 236 sec; M_∞ = 4.50; q_∞ = 43 954 Pa; α = 0.0605 rad;
T_{max} = 590.2 K; T_{avg} = 587.8 K; T_{min} = 581.7 K.

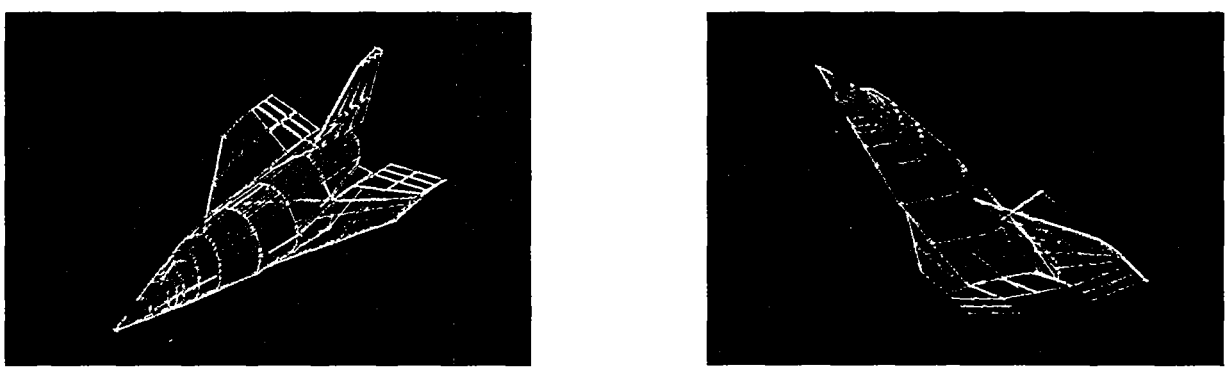

(ℓ) $t - t_i$ = 268 sec; M_∞ = 3.68; q_∞ = 31 362 Pa; α = 0.0605 rad;
T_{max} = 590.7 K; T_{avg} = 587.8 K; T_{min} = 572.0 K.

L-79-173

Figure 10.- Continued.

(m) $t - t_i$ = 308 sec; M_∞ = 3.00; q_∞ = 25 855 Pa; α = 0.0605 rad;
T_{max} = 588.9 K; T_{avg} = 576.7 K; T_{min} = 539.1 K.

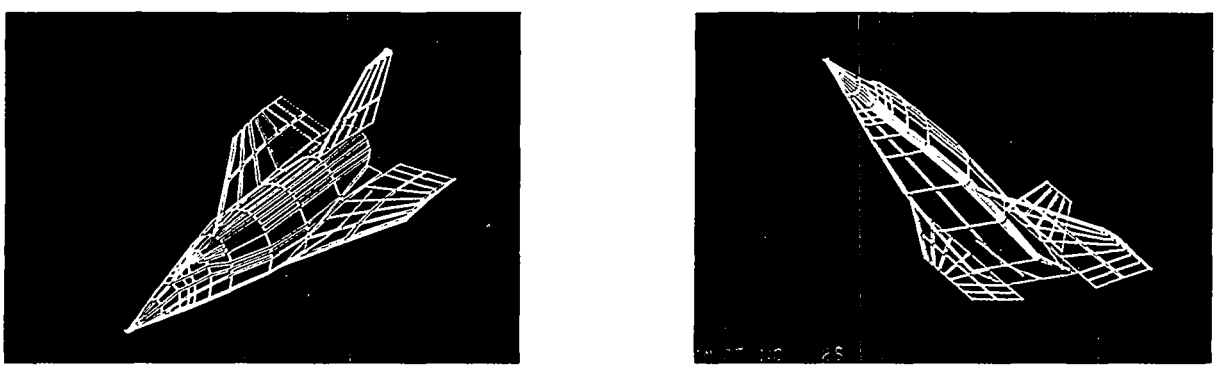

(n) $t - t_i$ = 348 sec; M_∞ = 2.38; q_∞ = 26 813 Pa; α = 0.0605 rad;
T_{max} = 584.6 K; T_{avg} = 552.3 K; T_{min} = 494.2 K.

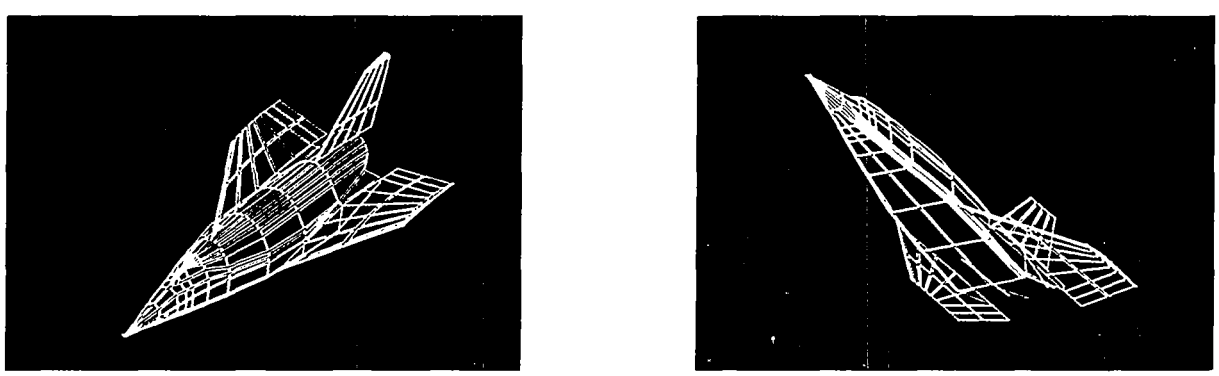

(o) $t - t_i$ = 372 sec; M_∞ = 2.00; q_∞ = 25 137 Pa; α = 0.0605 rad;
T_{max} = 581.0 K; T_{avg} = 534.8 K; T_{min} = 465.1 K.

L-79-174

Figure 10.- Concluded.

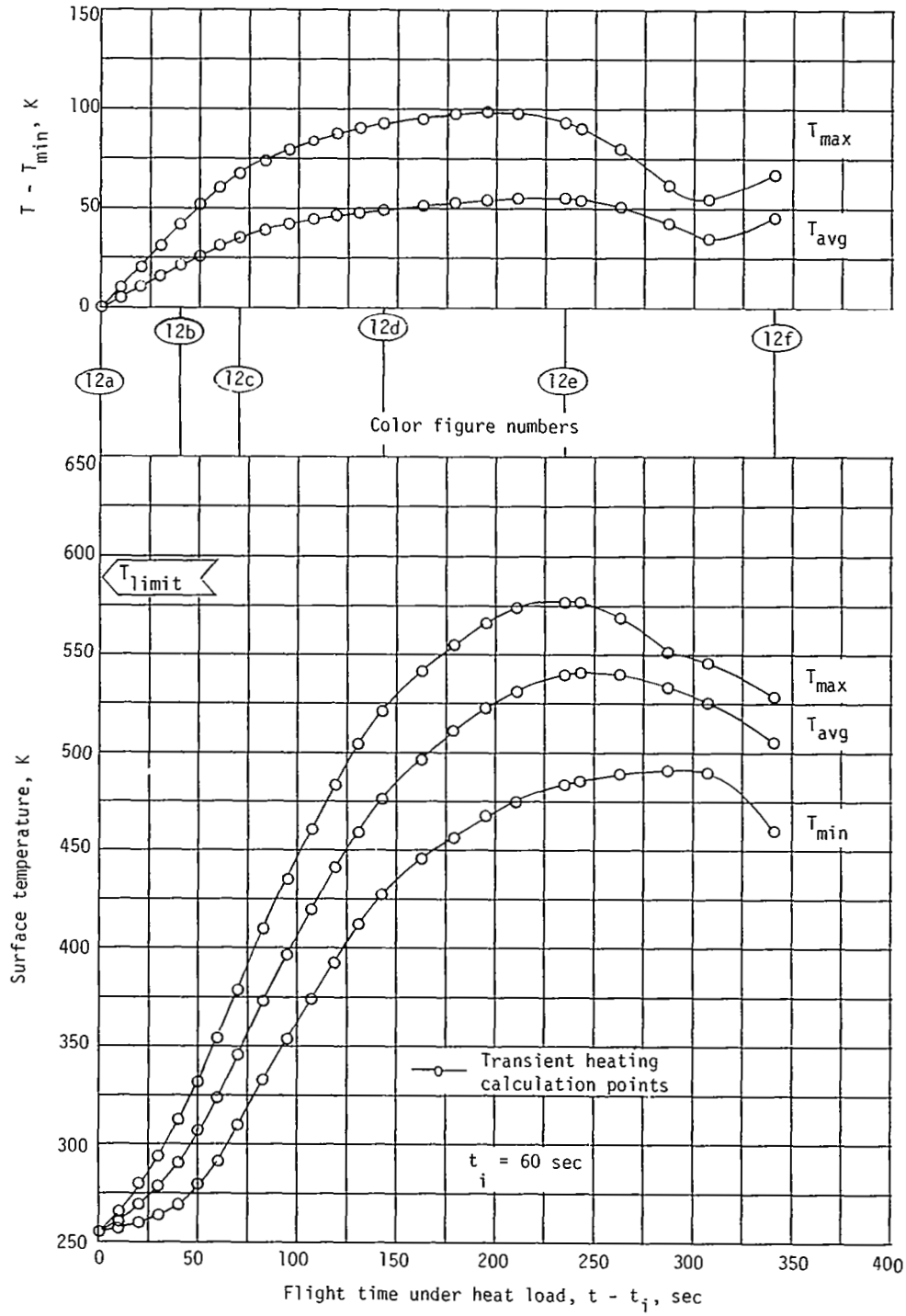

Figure 11.- Surface-temperature histories during 60 sec of cruise at Mach 6 mission using Lockalloy heat-sink TPS sized for maximum Mach number (M_{max} = 8.8) dash mission.

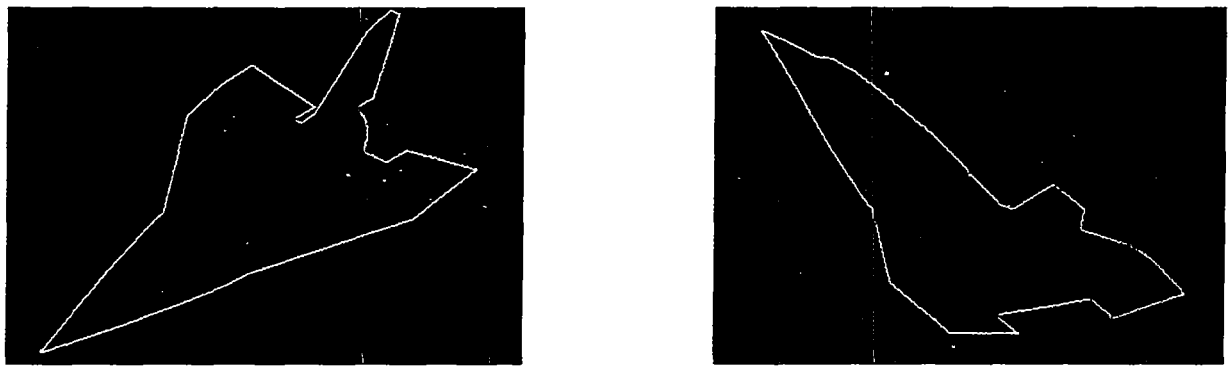

(a) $t - t_i$ = 0 sec; M_∞ = 2.00; q_∞ = 17 184 Pa; α = 0.0726 rad;
T_{max} = 255.6 K; T_{avg} = 255.6 K; T_{min} = 255.6 K.

(b) $t - t_i$ = 40 sec; M_∞ = 3.92; q_∞ = 24 740 Pa; α = 0.0726 rad;
T_{max} = 312.5 K; T_{avg} = 291.6 K; T_{min} = 270.8 K.

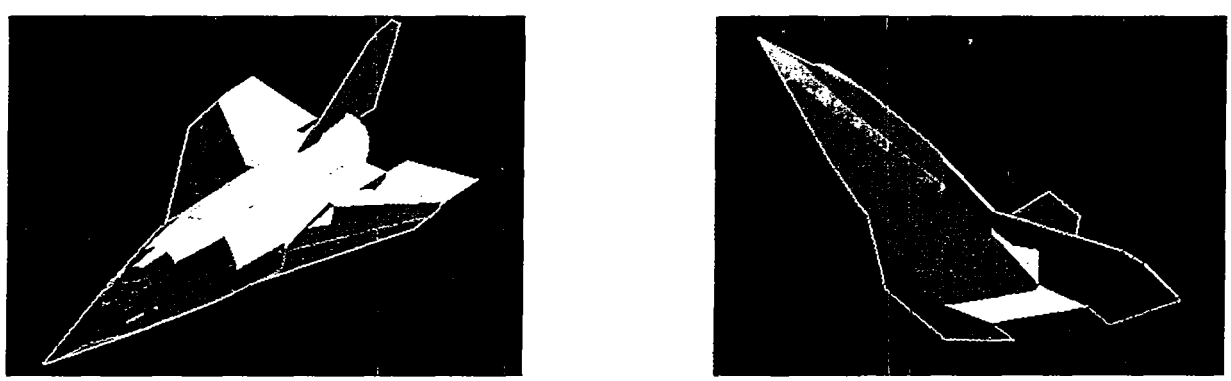

(c) $t - t_i$ = 71 sec; M_∞ = 6.00; q_∞ = 47 880 Pa; α = 0.0798 rad;
T_{max} = 381.6 K; T_{avg} = 348.8 K; T_{min} = 313.3 K.

L-79-175

Figure 12.- Color-coded raster graphics images with 7-color matrix representing surface-temperature gradients during 60 sec of cruise at Mach 6 mission using Lockalloy heat-sink TPS sized for maximum Mach number (M_{max} = 8.8) dash mission.

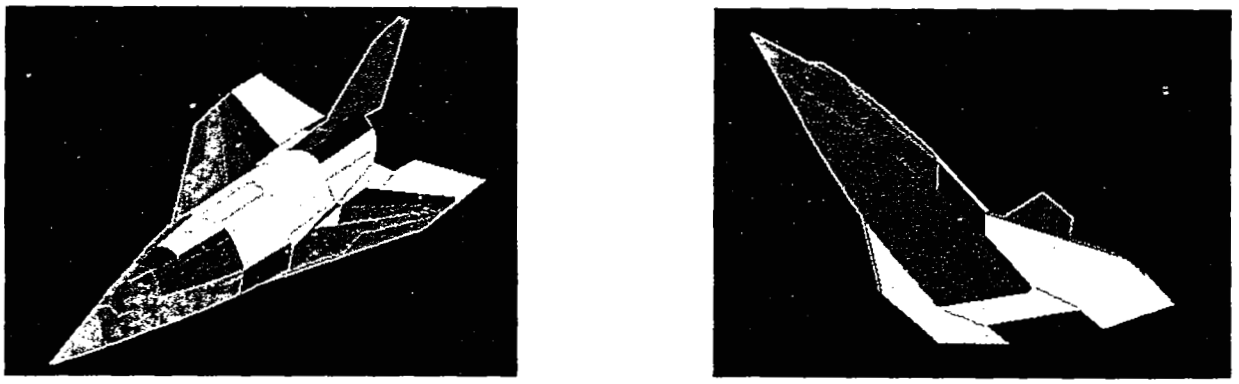

(d) $t - t_i$ = 143 sec; M_∞ = 5.69; q_∞ = 43 159 Pa; α = 0.0783 rad; T_{max} = 520.1 K; T_{avg} = 476.1 K; T_{min} = 427.1 K.

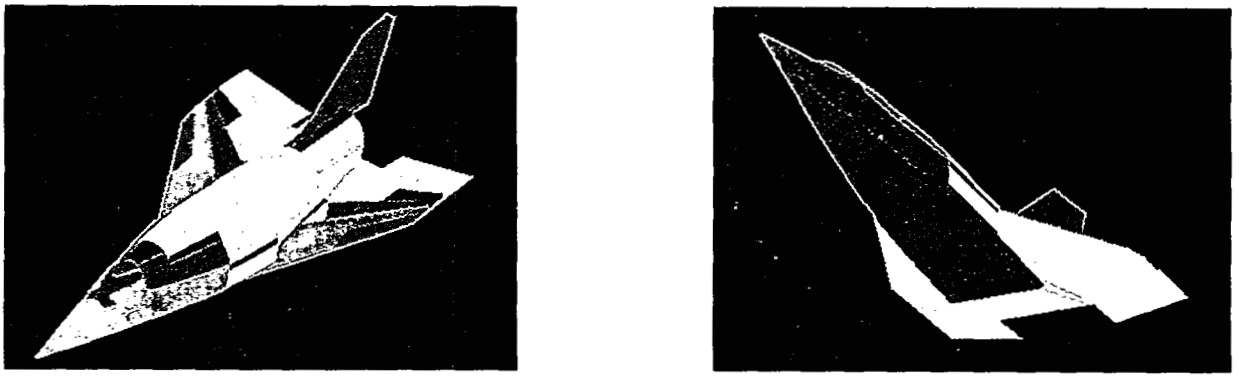

(e) $t - t_i$ = 235 sec; M_∞ = 3.89; q_∞ = 35 336 Pa; α = 0.0783 rad; T_{max} = 575.8 K; T_{avg} = 537.9 K; T_{min} = 483.2 K.

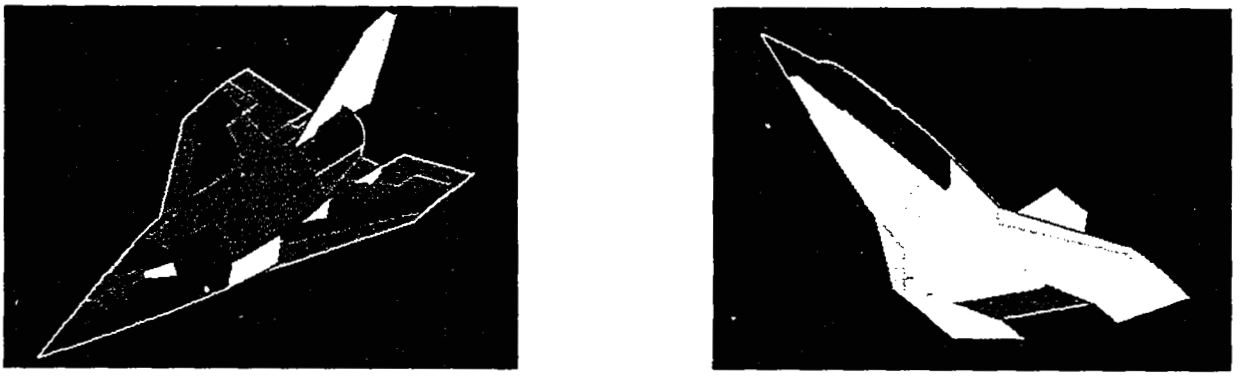

(f) $t - t_i$ = 341 sec; M_∞ = 2.00; q_∞ = 20 220 Pa; α = 0.0783 rad; T_{max} = 527.7 K; T_{avg} = 505.6 K; T_{min} = 460.7 K.

L-79-176

Figure 12.- Concluded.

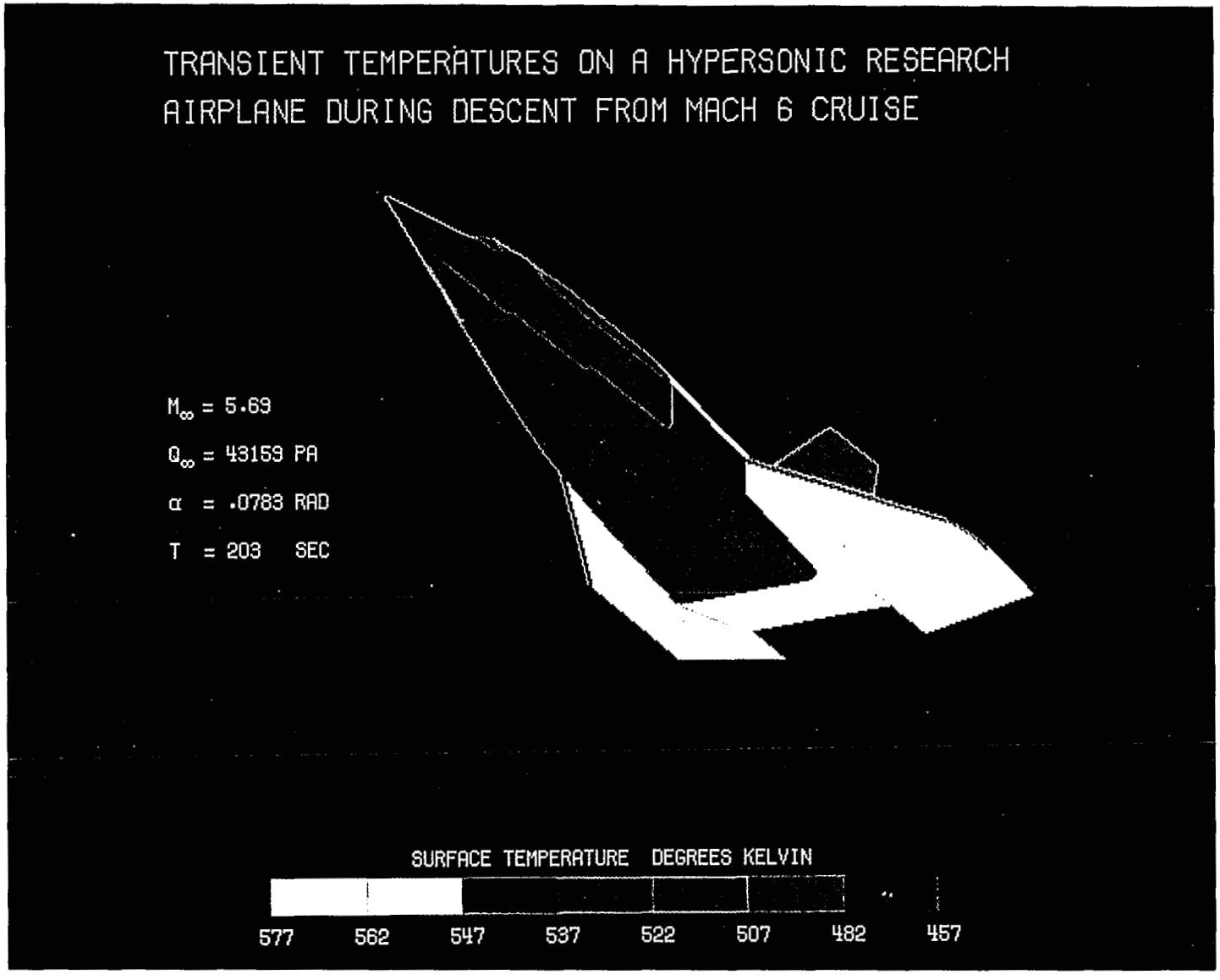

L-79-17

Figure 13.- Illustration of heating-panel and surface-temperature-gradient resolution available with increased image size.

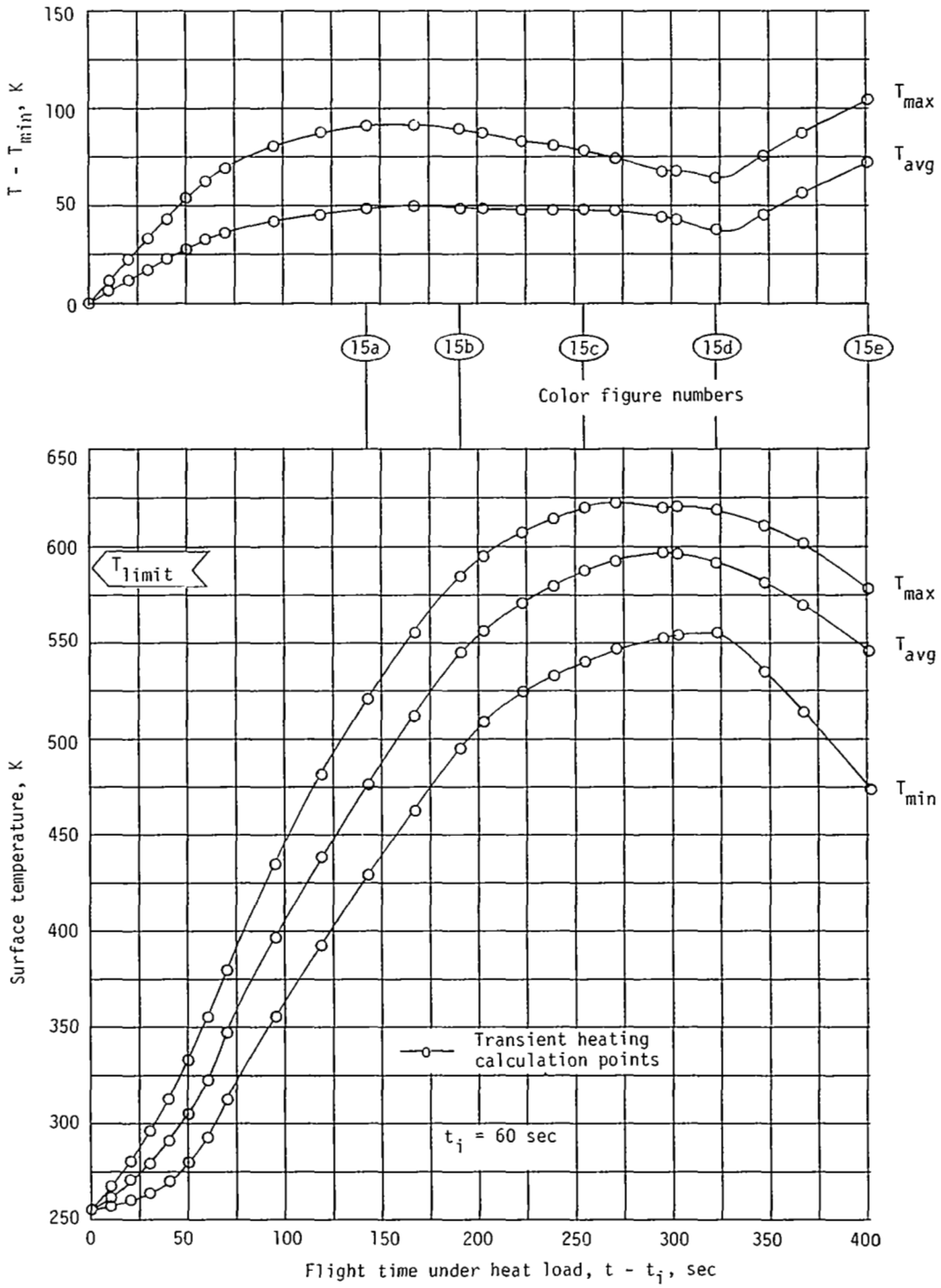

Figure 14.- Surface-temperature histories during 120 sec of cruise at Mach 6 mission using Lockalloy heat-sink TPS sized for maximum Mach number (M_{max} = 8.8) dash mission.

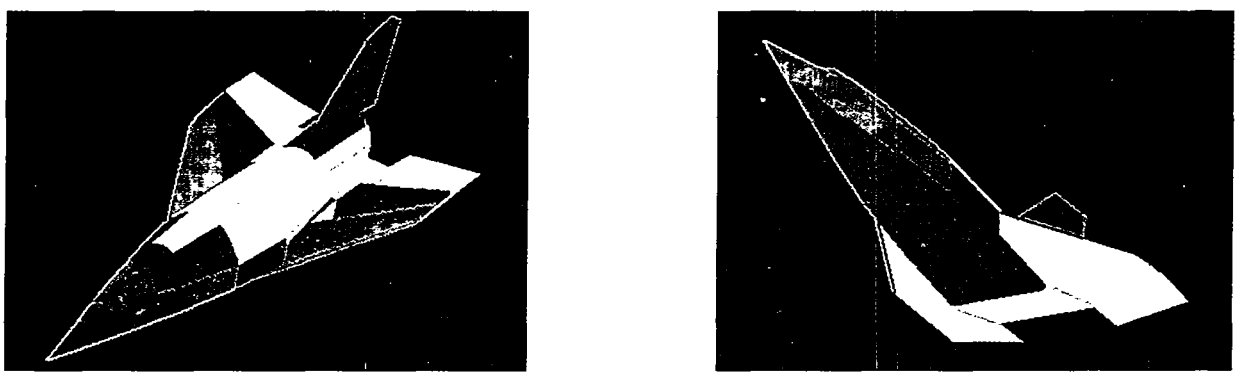

(a) $t - t_i$ = 143 sec; M_∞ = 6.00; q_∞ = 47 880 Pa; α = 0.0789 rad;
T_{max} = 519.4 K; T_{avg} = 476.2 K; T_{min} = 428.4 K.

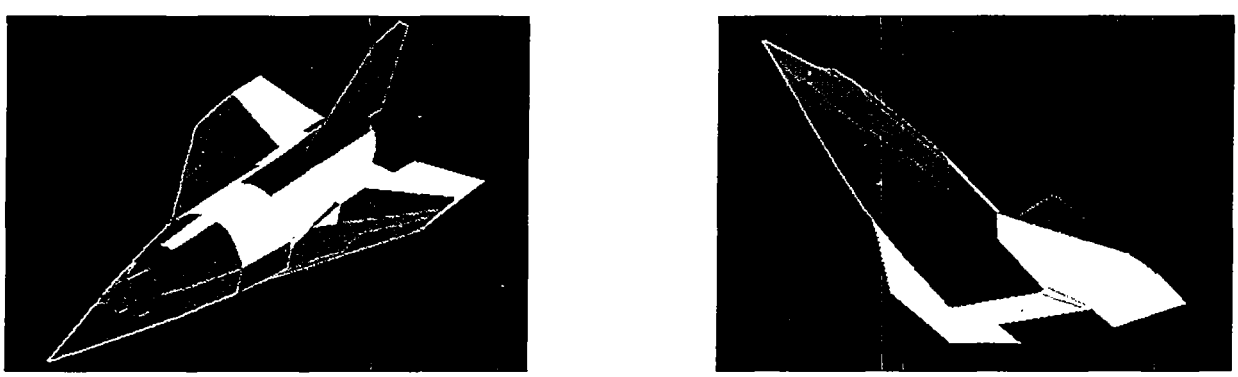

(b) $t - t_i$ = 191 sec; M_∞ = 6.00; q_∞ = 47 880 Pa; α = 0.0783 rad;
T_{max} = 582.9 K; T_{avg} = 542.3 K; T_{min} = 494.0 K.

L-79-178

Figure 15.- Color-coded raster graphics images with 7-color matrix representing surface-temperature gradients during 120 sec of cruise at Mach 6 mission using Lockalloy heat-sink TPS sized for maximum Mach number (M_{max} = 8.8) dash mission.

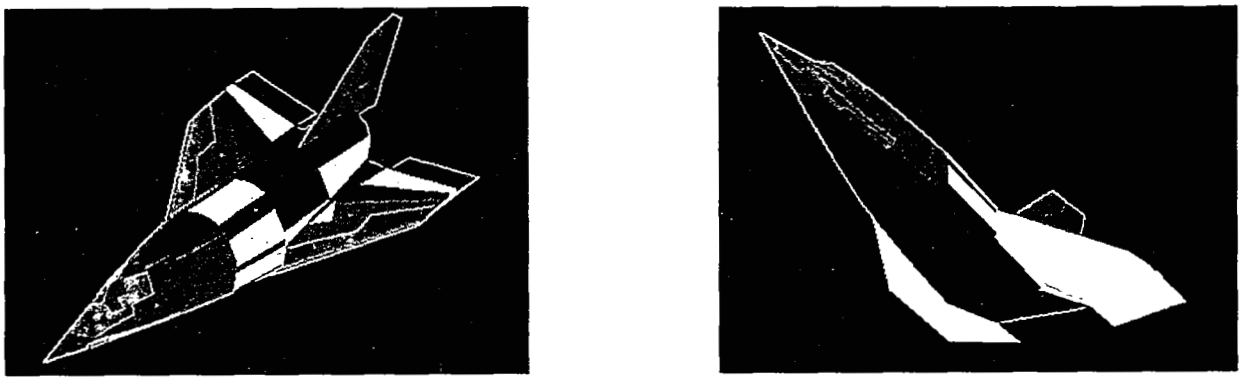

(c) $t - t_i$ = 255 sec; M_∞ = 4.62; q_∞ = 34 656 Pa; α = 0.0783 rad;
T_{max} = 617.4 K; T_{avg} = 586.2 K; T_{min} = 539.0 K.

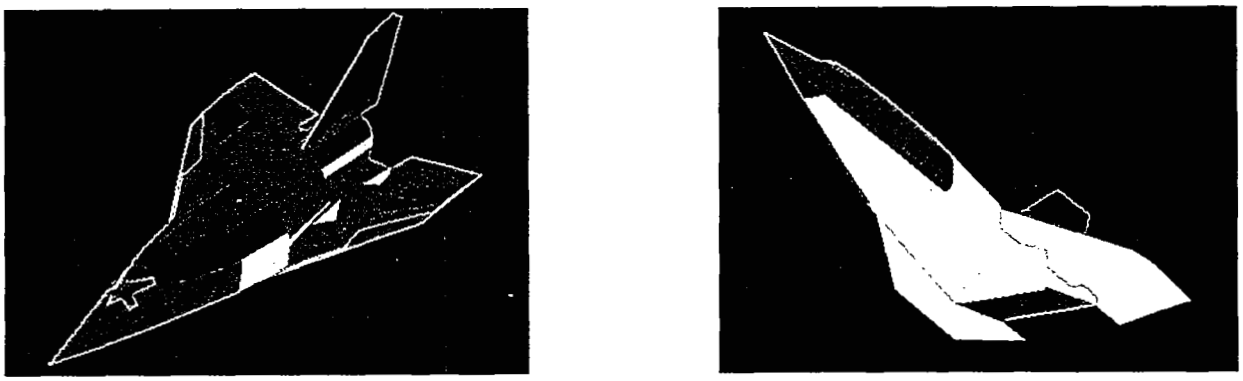

(d) $t - t_i$ = 323 sec; M_∞ = 3.35; q_∞ = 33 095 Pa; α = 0.0783 rad;
T_{max} = 617.1 K; T_{avg} = 590.0 K; T_{min} = 553.3 K.

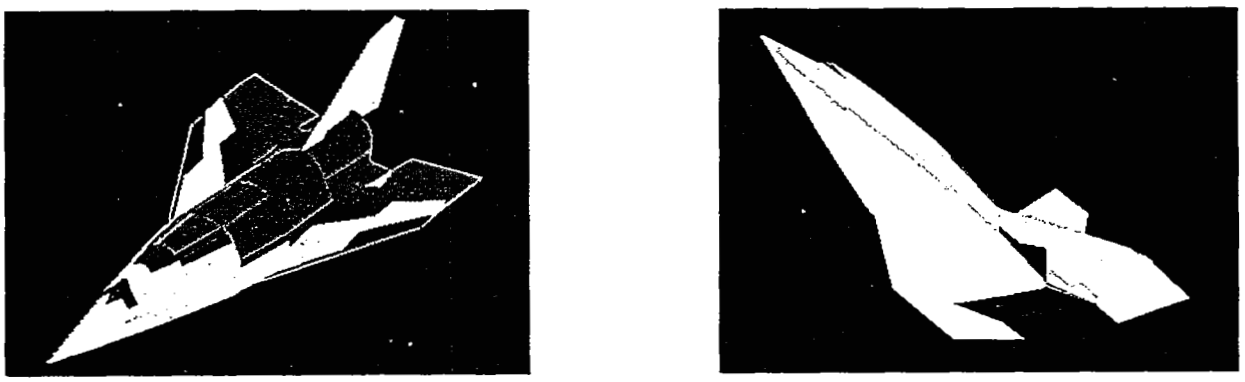

(e) $t - t_i$ = 401 sec; M_∞ = 2.00; q_∞ = 20 220 Pa; α = 0.0783 rad;
T_{max} = 577.4 K; T_{avg} = 544.8 K; T_{min} = 473.0 K.

L-79-179

Figure 15.- Concluded.

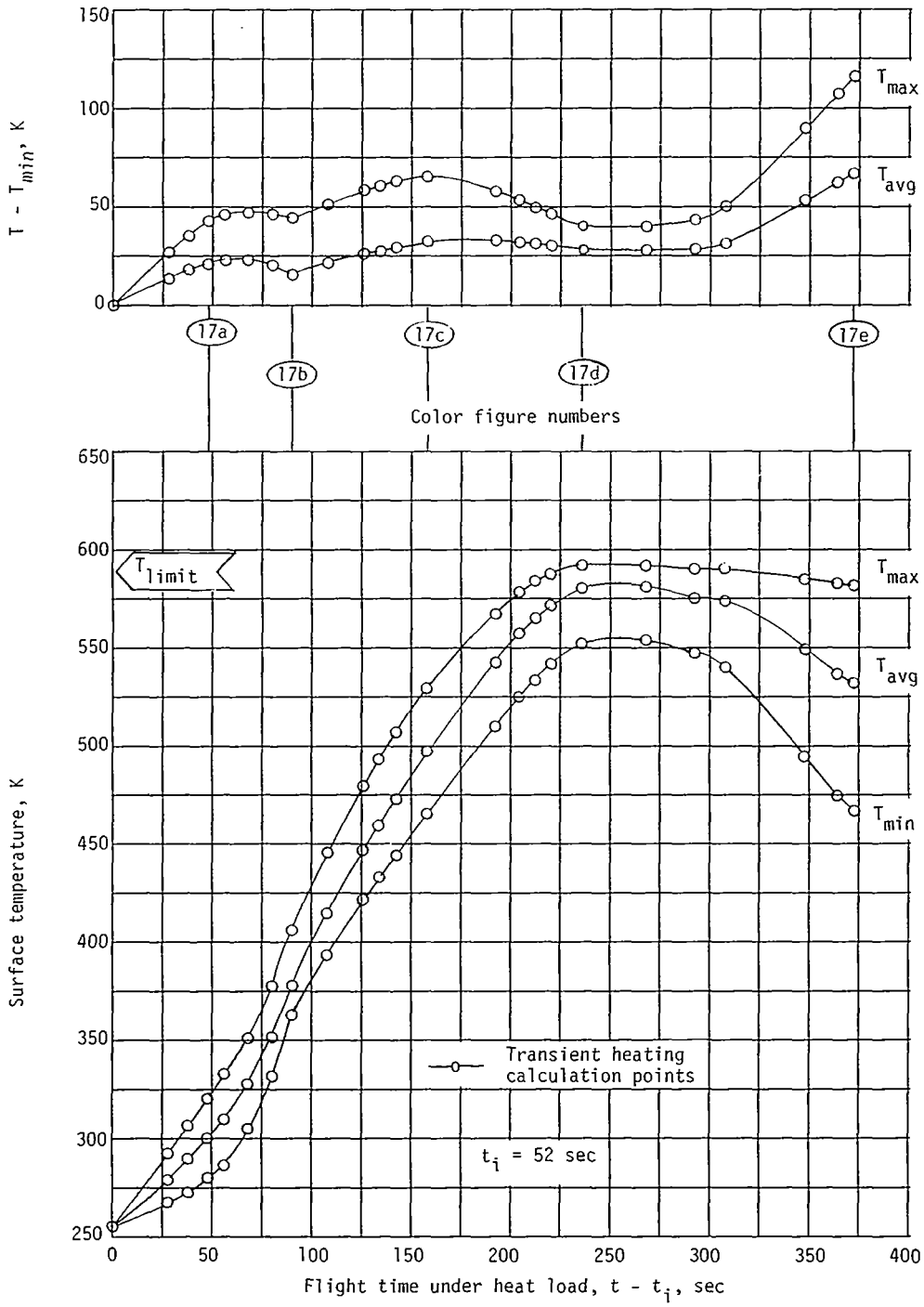

Figure 16.- Surface-temperature histories during maximum Mach number (M_{max} = 8.8) dash mission using Lockalloy heat-sink TPS sized for both the dash mission and the 120 sec of cruise at Mach 6 mission.

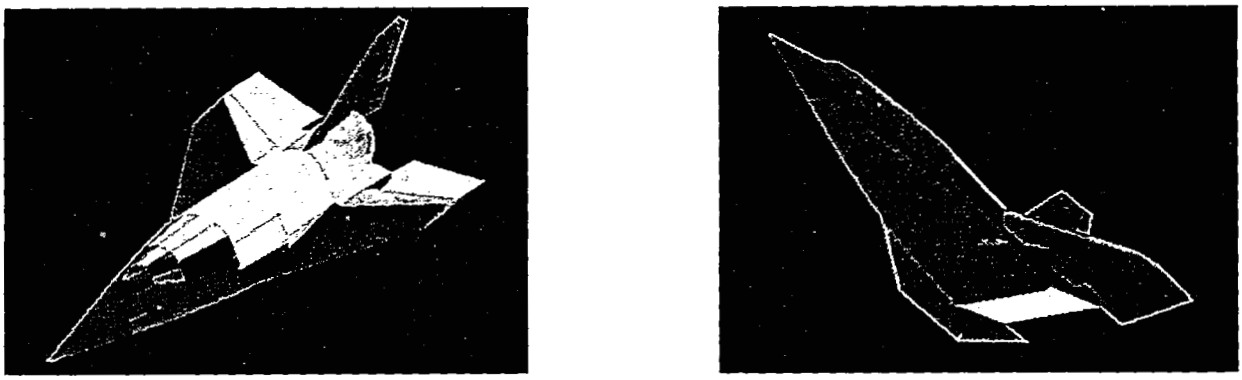

(a) $t - t_i$ = 48 sec; M_∞ = 4.82; q_∞ = 20 445 Pa; α = 0.0679 rad; T_{max} = 321.3 K; T_{avg} = 300.2 K; T_{min} = 279.8 K.

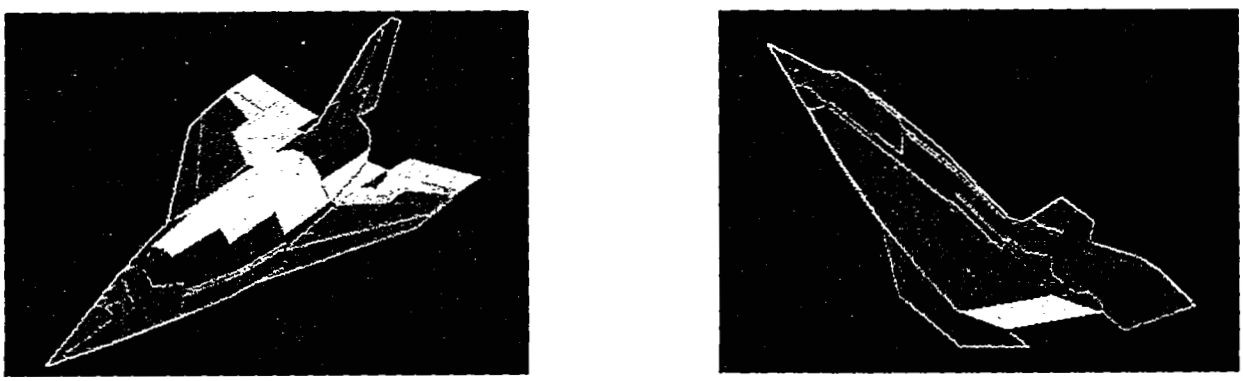

(b) $t - t_i$ = 90 sec; M_∞ = 8.78; q_∞ = 47 880 Pa; α = 0.0670 rad; T_{max} = 405.3 K; T_{avg} = 377.1 K; T_{min} = 362.2 K.

L-79-180

Figure 17.- Color-coded raster graphics images with 15-color matrix representing surface-temperature gradients during maximum Mach number (M_{max} = 8.8) dash mission using Lockalloy heat-sink TPS sized for both the dash mission and the 120 sec of cruise at Mach 6 mission.

(c) $t - t_i$ = 158 sec; M_∞ = 6.90; q_∞ = 42 278 Pa; α = 0.0605 rad;
T_{max} = 527.6 K; T_{avg} = 495.8 K; T_{min} = 463.4 K.

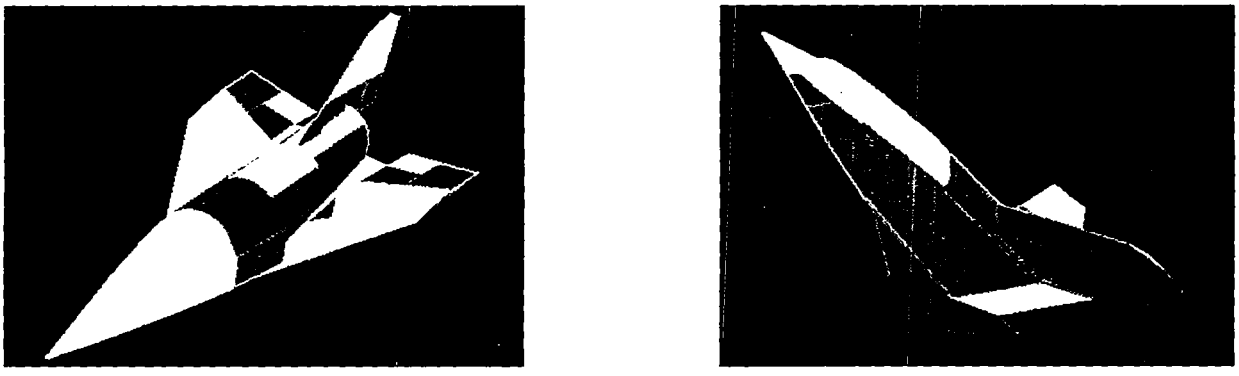

(d) $t - t_i$ = 236 sec; M_∞ = 4.50; q_∞ = 43 954 Pa; α = 0.0605 rad;
T_{max} = 590.1 K; T_{avg} = 578.9 K; T_{min} = 550.9 K.

(e) $t - t_i$ = 372 sec; M_∞ = 2.00; q_∞ = 25 137 Pa; α = 0.0605 rad;
T_{max} = 581.0 K; T_{avg} = 530.9 K; T_{min} = 465.1 K.

L-79-181

Figure 17.- Concluded.

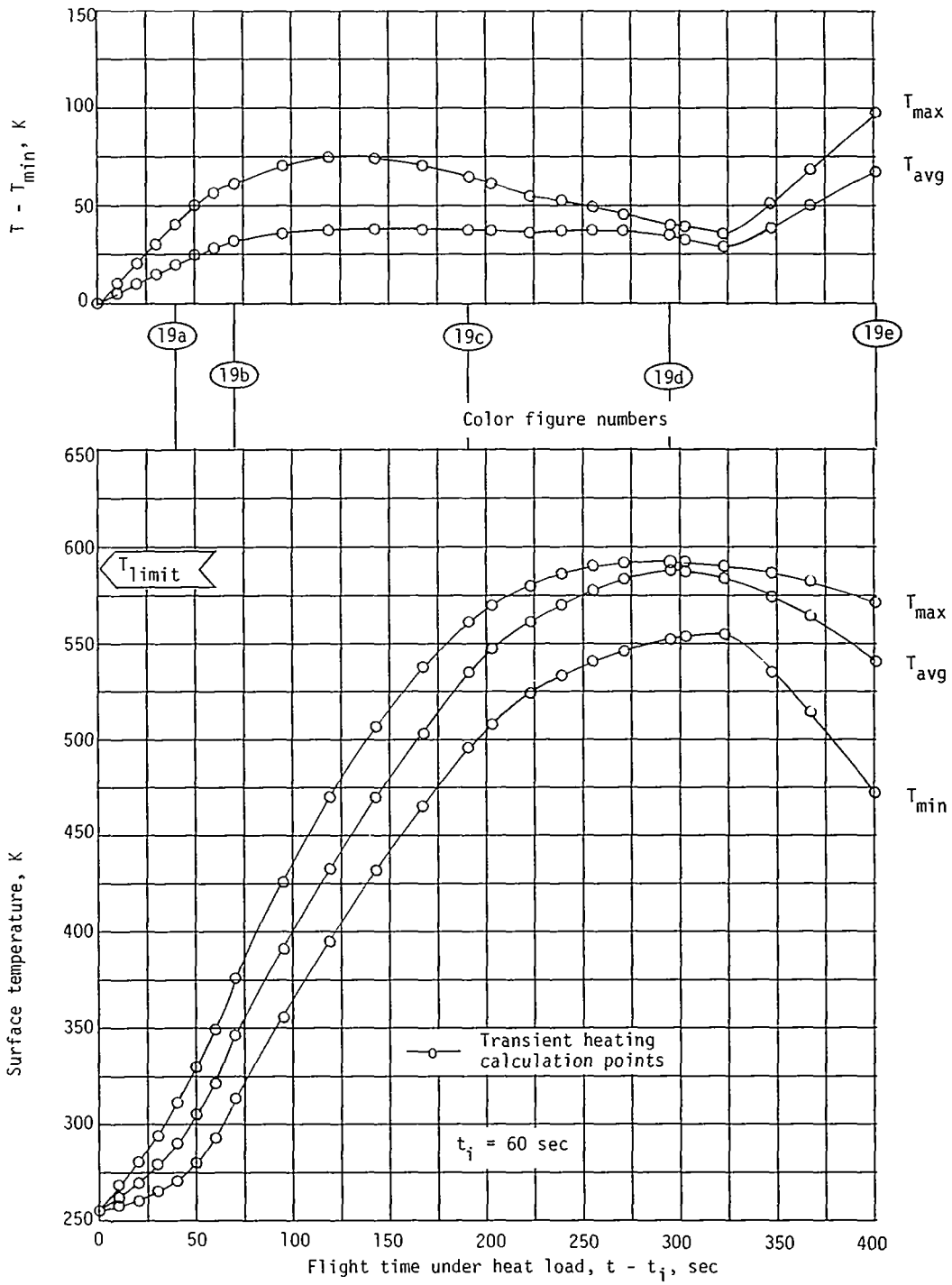

Figure 18.- Surface-temperature histories during 120 sec of cruise at Mach 6 mission using Lockalloy heat-sink TPS sized for both the maximum Mach number (M_{max} = 8.8) dash mission and the 120 sec of cruise mission.

(a) $t - t_i$ = 40 sec; M_∞ = 3.92; q_∞ = 24 740 Pa; α = 0.0726 rad; T_{max} = 310.3 K; T_{avg} = 290.1 K; T_{min} = 270.9 K.

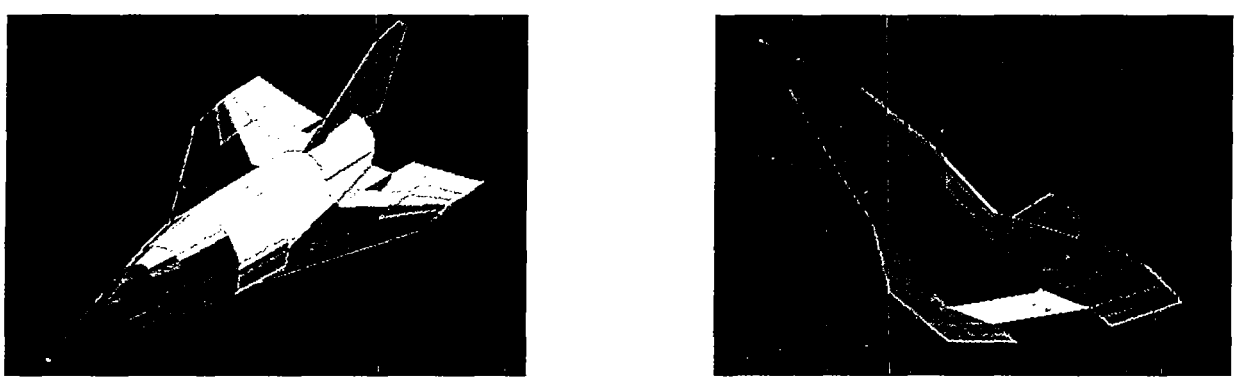

(b) $t - t_i$ = 71 sec; M_∞ = 6.00; q_∞ = 47 880 Pa; α = 0.0798 rad; T_{max} = 375.2 K; T_{avg} = 345.2 K; T_{min} = 313.9 K.

L-79-182

Figure 19.- Color-coded raster graphics images with 15-color matrix representing surface-temperature gradients during 120 sec of cruise at Mach 6 mission using Lockalloy heat-sink TPS sized for both the maximum Mach number (M_{max} = 8.8) dash mission and the 120 sec of cruise mission.

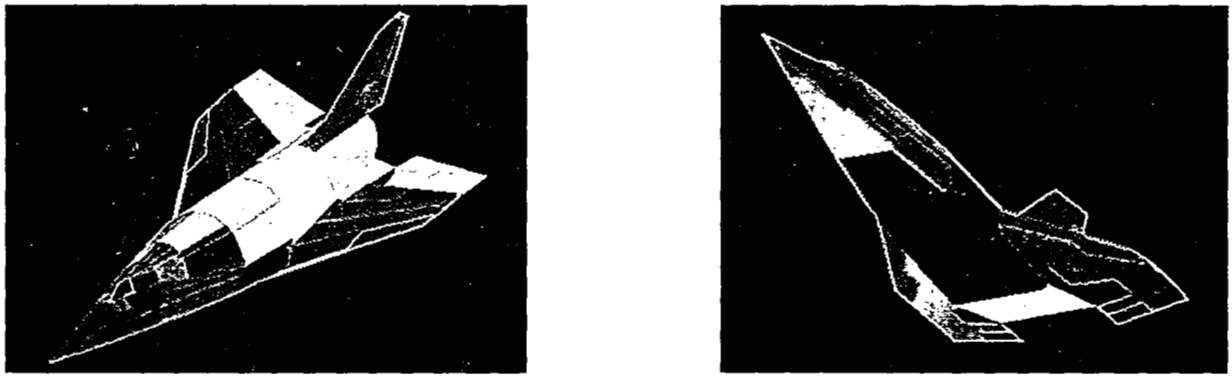

(c) $t - t_i$ = 191 sec; M_∞ = 6.00; q_∞ = 47 880 Pa; α = 0.0783 rad; T_{max} = 559.8 K; T_{avg} = 533.0 K; T_{min} = 495.2 K.

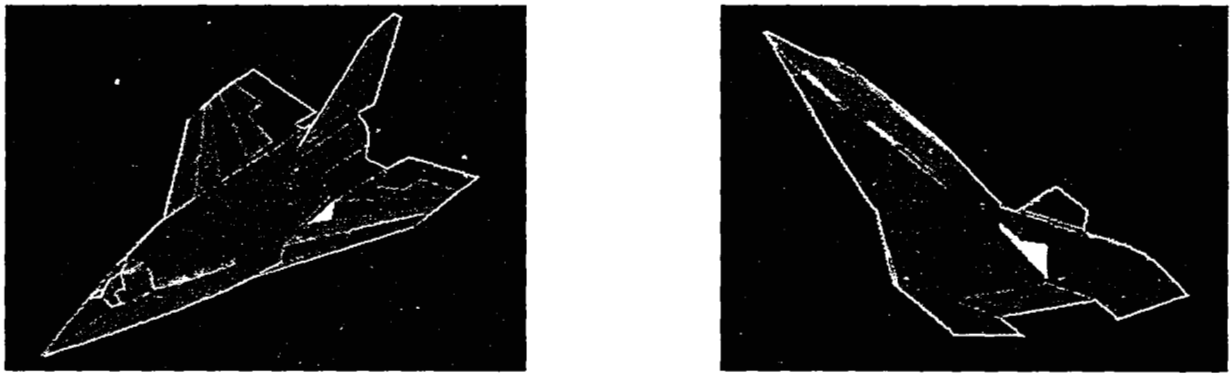

(d) $t - t_i$ = 295 sec; M_∞ = 3.89; q_∞ = 35 336 Pa; α = 0.0783 rad; T_{max} = 590.5 K; T_{avg} = 585.4 K; T_{min} = 550.9 K.

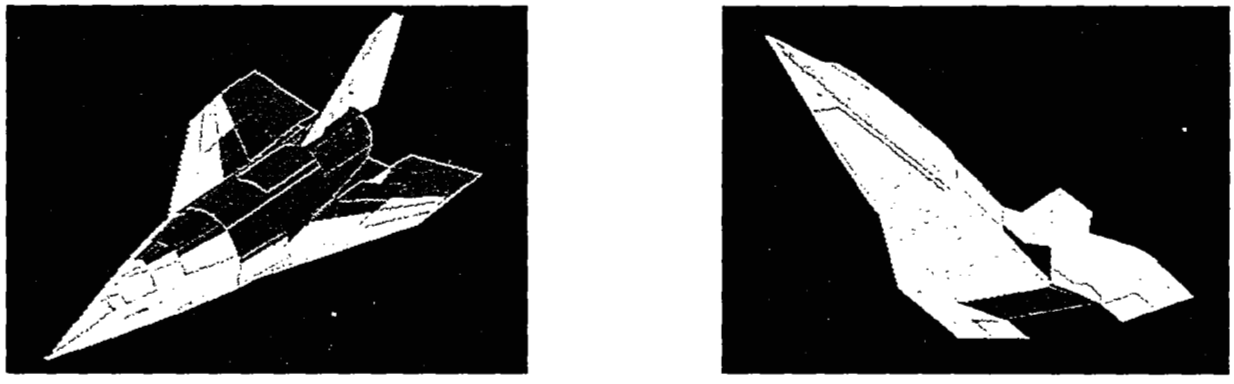

(e) $t - t_i$ = 401 sec; M_∞ = 2.00; q_∞ = 20 220 Pa; α = 0.0783 rad; T_{max} = 570.4 K; T_{avg} = 540.6 K; T_{min} = 472.7 K.

L-79-183

Figure 19.- Concluded.

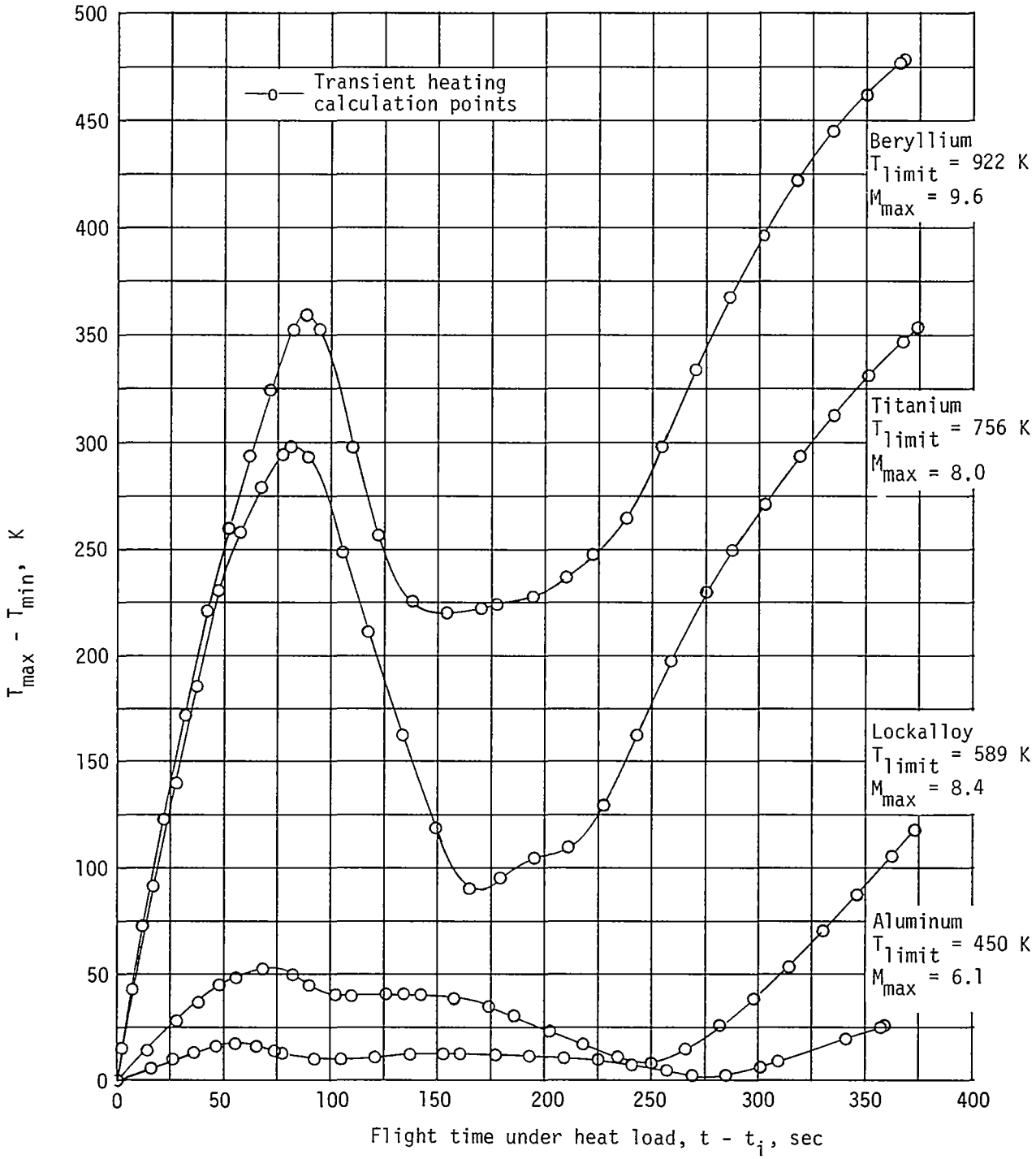

Figure 20.- Deviation in surface temperature of various skin materials during maximum Mach number dash missions.

1. Report No.	2. Government Accession No.	3. Recipient's Catalog No.
NASA TP-1455		

4. Title and Subtitle	5. Report Date
THE USE OF COMPUTER-GENERATED COLOR GRAPHIC IMAGES FOR TRANSIENT THERMAL ANALYSIS	July 1979
	6. Performing Organization Code
7. Author(s)	8. Performing Organization Report No.
C. L. W. Edwards, Frances T. Meissner, and James B. Hall	L-12779
	10. Work Unit No. 505-11-33-01
9. Performing Organization Name and Address	11 Contract or Grant No.
NASA Langley Research Center Hampton, VA 23665	
	13. Type of Report and Period Covered
12. Sponsoring Agency Name and Address	Technical Paper
National Aeronautics and Space Administration Washington, DC 20546	14. Sponsoring Agency Code

15. Supplementary Notes

16. Abstract

Color computer graphics techniques were investigated as a means of rapidly scanning and interpreting large sets of transient heating data. The data presented in this paper were generated to support the conceptual design of a heat-sink thermal protection system (TPS) for a hypersonic research airplane. Color-coded vector and raster displays of the numerical geometry used in the heating calculations were employed to analyze skin thicknesses and surface temperatures of the heat-sink TPS under a variety of trajectory flight profiles. Both vector and raster displays proved to be effective means for rapidly identifying heat-sink mass concentrations, regions of high heating, and potentially adverse thermal gradients. The color-coded (raster) surface displays are a very efficient means for displaying surface-temperature and heating histories, and thereby the more stringent design requirements can quickly be identified. The related hardware and software developments required to implement both the vector and the raster displays for this application are also discussed.

17. Key Words (Suggested by Author(s))	18. Distribution Statement
Hypersonic Aerodynamic heating Color graphics Thermal protection	Unclassified - Unlimited Subject Category 34

19. Security Classif. (of this report)	20. Security Classif. (of this page)	21. No. of Pages	22. Price*
Unclassified	Unclassified	44	$4.50

* For sale by the National Technical Information Service, Springfield, Virginia 22161

1 1 1U,D, 062979 S00903DS
DEPT OF THE AIR FORCE
AF WEAPONS LABORATORY
ATTN: TECHNICAL LIBRARY (SUL)
KIRTLAND AFB NM 87117